

QUANTUM PROBABILITY: A NEW METHOD FOR MODELLING TRAVEL BEHAVIOUR

Thomas O. Hancock (Corresponding Author)

Choice Modelling Centre and Institute for Transport Studies
University of Leeds
tratoh@leeds.ac.uk

Jan Broekaert

Choice Modelling Centre and Institute for Transport Studies
University of Leeds
jan.b.broekaert@gmail.com

Stephane Hess

Choice Modelling Centre and Institute for Transport Studies
University of Leeds
S.Hess@its.leeds.ac.uk

Charisma F. Choudhury

Choice Modelling Centre and Institute for Transport Studies
University of Leeds
C.F.Choudhury@leeds.ac.uk

1 ABSTRACT

2 There has been an increasing effort to improve the behavioural realism of mathematical models of
3 choice, resulting in efforts to move away from random utility maximisation (RUM) models. Some
4 new insights have been generated with, for example, models based on random regret minimisation
5 (RRM, μ -RRM). Notwithstanding work using for example Decision Field Theory (DFT), many of
6 the alternatives to RUM tested on real-world data have however only looked at only modest de-
7 partures from RUM, and differences in results have consequently been small. In the present study,
8 we address this research gap again by investigating the applicability of models based on quantum
9 theory. These models, which are substantially different from the state-of-the-art choice modelling
10 techniques, emphasise the importance of contextual effects, state dependence, interferences and
11 the impact of choice or question order. As a result, quantum probability models have had some
12 success in better explaining several phenomena in cognitive psychology. In this paper, we con-
13 sider how best to operationalise quantum probability into a choice model. Additionally, we test
14 the quantum model frameworks on a best/worst route choice dataset and demonstrate that they find
15 useful transformations to capture differences between the attributes important in a most favoured
16 alternative compared to that of the least favoured alternative. Similar transformations can also be
17 used to efficiently capture contextual effects in a dataset where the order of the attributes and al-
18 ternatives are manipulated. Overall, it appears that models incorporating quantum concepts hold
19 significant promise in improving the state-of-the-art travel choice modelling paradigm through
20 their adaptability and efficient modelling of contextual changes.

1 1. INTRODUCTION

2 The random utility maximisation (RUM) framework has dominated the travel choice modelling
3 field for many decades. More recently, RUM has been criticised as being inadequate in explain-
4 ing the full range of behavioural complexity (Chorus et al., 2008; Guevara and Fukushi, 2016).
5 This has resulted in many attempts to better incorporate behavioural concepts into travel behaviour
6 models, including regret (Chorus et al., 2008; Chorus, 2010), contextual relative advantages (Leong
7 and Hensher, 2014) and prospect theory (Avineri and Bovy, 2008). However, none of these de-
8 velopments have yet rivalled RUM as the preferred model in real-world applications. This is due
9 to difficulties that quickly arise once a modeller departs from the firm economic foundations of
10 RUM (Hess et al., 2018). Consequently, caution is required if we are to step away from random
11 utility models. Departures to models with similar underlying structures, i.e. those with the same
12 error structure such as random regret minimisation (Chorus et al., 2008; Chorus, 2010), result in
13 only small differences whilst facing the same key disadvantage of all departures from (linear in
14 attribute) RUM, the loss of the ability to calculate welfare measures (for a further discussion on
15 welfare analysis with non-linear effects, see e.g. Batley and Dekker (2019) and for regret models,
16 see Dekker 2014). Departures to more different models, such as decision field theory (Busemeyer
17 and Townsend, 1992), whilst sometimes finding improvements in model fit, additionally result
18 in models that become computationally infeasible for large-scale datasets (Hancock et al., 2018).
19 Thus, if we are to move away from RUM, we need to investigate alternative approaches that are
20 computationally simpler yet better reflect behavioural realism. This leads us to explore and com-
21 pare dynamical modelling ideas from other disciplines which are further away from the tried and
22 tested. Given the success of using concepts from quantum physics in cognitive psychology, one
23 possible alternative is to see if quantum physics can make a similar step into travel behaviour
24 modelling. A fundamental aspect of quantum-like models is that they are intrinsically probabilis-
25 tic. While in, for example, RUM and RRM, a stochastic sampling of the utility function is added
26 to the model to produce probabilistic output, a quantum-like choice model instead implements the
27 stochasticity at the foundation of the decision process *in the mind of the individual decision-maker*.

28 Quantum physics, first considered in the early 20th century, was originally developed to ac-
29 count for phenomena and results that could not be explained by classical theories of probability
30 and physics. In particular, physicists noticed that the measurement of one variable could impact the
31 measurement of another. One of the archetypal experiments of quantum mechanics is the double-
32 slit scattering experiment (Feynman et al., 1965). In this experiment, either a beam of light or
33 particles is projected on a screen with two fine parallel slits. Further behind the slit-screen, the
34 intensity of the scattered beam is measured across the receptor screen, in the same direction as the
35 slits are separated (Figure 1). When light waves are applied in this experiment, an intensity pattern
36 emerges on the receptor screen which shows both diffraction, caused by light scattering within
37 each slit, and interference, caused by compounding the light waves coming from the two differ-
38 ent slits. The major surprise comes from the fact that these same patterns also occur for beams
39 of material particles - e.g. neutrons or heavy molecules. Even when the source is so scarce that
40 one can legitimately assume that only a single particle at once crosses the two slits, a diffraction
41 and interference pattern will still over time build up on the detection screen. Not only does the
42 double-slit experiment prove that matter behaves as waves, but it also shows that a single particle
43 can have non-compatible properties - like being at different locations A and B at the same time.
44 This potential for ‘non-locality’ of a particle ensues the particle must be at position A and B at the
45 same time in order to produce wave-like interference pattern over the positions C on the detector

1 screen (Figure 1). It has been shown that as soon as the presence of the particle at either of the slits
 2 is positively confirmed for sure, the interference pattern on the detection screen disappears.¹

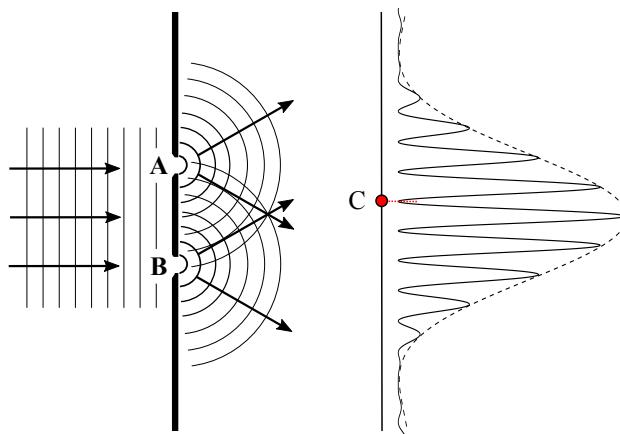


FIGURE 1 : The double-slit experiment (top view). Plain waves are scattered through the double-slit screen (A and B) and produce a diffraction and interference pattern of intensity on the detection screen (C, located at a zero point of the intensity). The dashed line indicates the intensity resulting from single-slit diffraction.

3 In the double-slit experiment, we can measure for the outcome of the (statistical) propositions
 4 $\{a, b, c\}$.

5 a : ‘the particle is present at A’

6 b : ‘the particle is present at B’

7 c : ‘the particle is *never* present at C’ (C is at a zero-point of the interference pattern)

8 Let us suppose single particles repeatedly and individually enter the double-slit device (proposition
 9 a or b is true) and we do not observe a particle at C (proposition c is true). Then the outcomes
 10 for $(a \vee b)$ and c are both true. Then, by the distributivity law of classical logic, this means that
 11 $((c \wedge a) \vee (c \wedge b))$ is also **true**. However, if we evaluate these two expressions according to the
 12 procedures of quantum probability, they both are false. First, the proposition $(c \wedge a)$ is false because
 13 the procedure shows a particle is never observed at C if we have an affirmative observation of the
 14 particle at A, while a non-observation of the particle at location A must set the particle affirmatively
 15 at location B and again excludes proposition c . By the same token the $(c \wedge b)$ is false, since never
 16 observing a particle at C means the particle cannot have been observed at either of the slits. Thus,
 17 for this experiment, $(c \wedge a) \vee (c \wedge b)$ is **false**, an explicit contradiction of the outcome of $c \wedge (a \vee b)$.
 18 This particular example clearly exposes that the classical distributivity rule of ‘and’ and ‘or’ does
 19 not apply for non-compatible features in quantum theory.

20 These findings resulted in the creation of a new theory of probability, known as quantum logic
 21 (Birkhoff and Von Neumann, 1936). Under quantum logic (which is also known as quantum prob-
 22 ability), a new set of probability rules were defined, which crucially did not include the axiom of

¹See also Englert (1996) and Greenberger and Yasin (1988) for the expression of the gradual relation between interference visibility and position predictability.

1 distributivity. This new theory of probability has subsequently made the transition into cognitive
2 psychology (Bruza et al., 2015) and has also been introduced into transport behaviour modelling.
3 For example, Vitetta (2016) introduced a quantum model based on random utility models with
4 the addition of an interference term for route choice problems. Additionally, Yu and Jayakrish-
5 nan (2018) demonstrated that quantum cognition models can be used effectively to capture the
6 difference in state of mind between choices made under stated preference and revealed preference
7 settings. However, as far as the authors are aware, there has not been an actual choice model devel-
8 oped with quantum concepts that incorporates attribute values for individual alternatives and can
9 work for general choices as well as ‘changes in perspective’. Thus, the focus of this paper is to
10 explore ways to develop a choice modelling framework based on quantum probability theory that
11 can be used for choices in general, as well as efficiently capturing effects caused by ordering and
12 context, by engendering interference and rotation effects which adequately reflect the changes in
13 the ‘state of mind’ of the respondents.

14 In our present study, we will present two quantum models using distinct approaches. The first
15 model, named the ‘*amplitude model*’, is an innovative approach related to geometrically based
16 quantum-like models. In (all) quantum-like models the belief-action state of a respondent is de-
17 scribed by a vector in a Hilbert space. The amplitude components of the vector represent the latent
18 motivation to choose each of the alternatives. In essence, the ‘amplitude model’ implements the
19 expressions of utility (or regret) immediately in the amplitudes of the belief-action state of a re-
20 spondent. As such, the amplitude model puts the support for each of the alternatives in a trial
21 directly at the level of a measurable quantity, the probability (amplitude).

22 The second model, designated as the ‘*Hamiltonian model*’, is based on a dynamic principle
23 in which the change of the belief state results from attribute comparisons of the alternatives. In
24 this model, therefore, the ‘deliberation process’ itself is implemented. The dynamic approach to
25 quantum-like modelling uses the ‘energy operator’, or Hamiltonian, of quantum mechanics to im-
26 plement the change of the belief state over time. The changes are caused by the information in
27 (and effects from) the input, such as descriptions, questions and choice alternatives or other pre-
28 sented sensory resources (Pothos and Busemeyer, 2009; Atmanspacher and Filk, 2010; Martínez-
29 Martínez, 2014; White et al., 2014). In our present study the expressions of utility or regret are
30 implemented in the phenomenological Hamiltonian. This Hamiltonian then causes the evolution
31 of the initial belief-action state of the respondent towards the informed state in which the decision
32 is made.

33 The remainder of this paper is organised as follows. First, we introduce quantum probability
34 theory and discuss the relative benefits of using such a system. We then mathematically describe
35 quantum probability theory, discussing how it can be incorporated into a choice model and de-
36 tailing two different formulations for new models. We next test the performance of our proposed
37 models against typical choice models such as multinomial logit, random regret minimisation and
38 also decision field theory, in the context of travel decisions. Finally, we test the use of ‘quantum
39 rotations’ on best-worst and contextual choice data, before drawing some conclusions.

40 2. QUANTUM PROBABILITY THEORY

41 In this section, we first give a general overview of quantum probability theory. We then give
42 the mathematical definitions for how quantum probability theory works for basic choices. We
43 conclude by describing how it works for a series of related choices. It is in the transformation from
44 one choice task to another that a modelling framework based on quantum probability theory looks

1 very different from traditional choice models.

2 2.1. Overview of quantum probability theory

3 A simple example of how quantum probability theory works is given in Figure 2. Initially, a
 4 decision-maker might be making a single choice between two alternatives, travelling by car or by
 5 train. Each of these alternatives is represented by vectors, $|T\rangle$ and $|C\rangle$ respectively (the axes in
 6 Figure 2). Under quantum probability theory, the decision-maker has some belief state, denoted
 7 $|z\rangle$, regarding whether they will choose car or train.

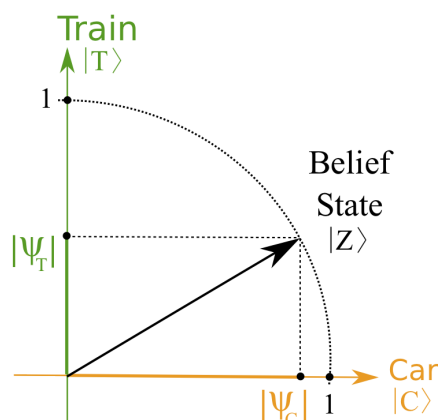


FIGURE 2 : Schematic representation of the belief state in the geometric quantum-like model for a binary choice ‘Train’ or ‘Car’. The belief state $|Z\rangle$ is a superposition of $|T\rangle$ and $|C\rangle$, expressing support for both the choice of Train and Car. The (modulus of the) complex-valued amplitudes of the projections on the respective axes provides the probabilities of each alternative by squaring the projection lengths $|\psi_T|$ and $|\psi_C|$. In this schematic representation, the units on the axes are reals and the normalised belief state is a point on the unit circle.²The cosine-similarity of the overall belief state and the ‘Train’ choice outcome is given by $|\psi_T| = |\langle T|Z\rangle|$.

8 The action of making a choice (or equivalently coming to some result or making a judgement)
 9 results in a reduction of the state. This can be represented graphically by projecting the belief state
 10 vector onto the vector corresponding to the chosen alternative. In this example, ψ_T , represents the
 11 scalar projection of $|z\rangle$ onto the unambiguous state $|T\rangle$ for choosing the train. The ‘length’ of this
 12 projection is then denoted $|\psi_T|$. In Figure 2, these projections are directly over the corresponding
 13 vectors, and on the axes we denoted the norm of the respective amplitudes.

14 For example, when the belief state vector is at 45 degrees (with respect to the Car and Train
 15 axes), the two projections are of equal length and the choice probabilities are thus 50% each. In the
 16 example in Figure 2, the car alternative has a higher probability since it shows a larger amplitude
 17 than the train component. The full mathematical description for this is given in the following
 18 section on a basic choice under quantum probability theory, which also gives a 3-dimensional
 19 example. The ‘longer’ the projection onto the vector for an alternative, the more likely it is for
 20 that alternative to be chosen. The crucial difference in using such a system is how an additional
 21 question or nudge can impact the decision-maker’s choice for the first question (car or train). If,

²This schematic representation should not be confused with the Bloch sphere representation for the spin-1/2 particle in quantum mechanics.

1 for example, the decision-maker was asked ‘are you environmentally friendly?’ before they had
 2 made up their mind between the choice of car or train, they would then be initially answering a
 3 different question and making a different choice. As a result of the decision-maker deciding ‘I am
 4 environmentally friendly’, the decision-maker’s state moves from the initial starting state and is
 5 projected onto the vector representing ‘environmentally friendly’ and vice versa if they decide ‘I
 6 am not environmentally friendly’ (see Figure 3). This results in making the choice between car
 7 and train from a different state. Consequently, the length of the projections ($|\psi_C|$ and $|\psi_T|$) onto
 8 the vectors for car and train have changed. This is graphically represented in Figure 3, with the
 9 projection length $|\psi_T|$ being longer if the initial state is first projected onto the environmentally
 10 friendly vector before being projected onto the train vector, relative to the projection length if train
 11 is chosen directly from the initial state. Consequently, the probabilities for choosing car and train
 12 are altered.

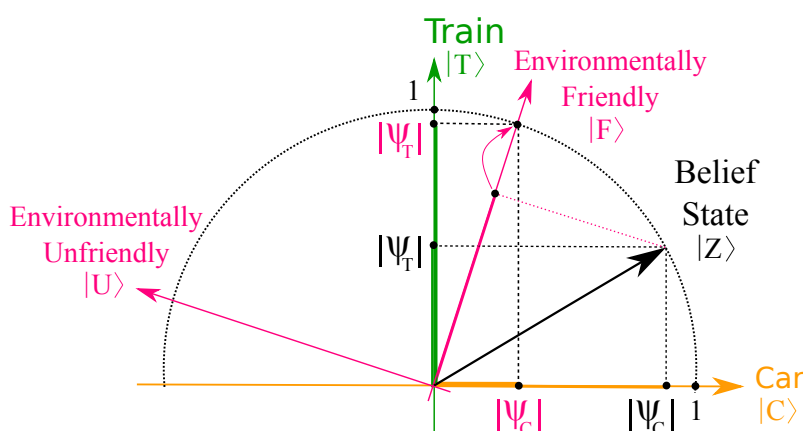


FIGURE 3 : Schematic representation of making two consecutive binary choices under quantum probability theory in the geometric quantum-like model; first ‘Environmentally friendly’ or ‘Environmentally unfriendly’, followed by ‘Train’ or ‘Car’. The preparatory ecological question recasts the belief state on the basis $\{|F\rangle, |U\rangle\}$ and will increase the belief support for the choice ‘Train’ on a *positive* outcome for ‘Environmentally Friendly’ since the amplitude norm $|\psi_T|$, in pink, is then larger than amplitude norm $|\psi_T|$, in black, and the reverse is true for ‘Car’. Notice that while the initial belief state $|Z\rangle$ only had some latent tendency for responding ‘Environmentally Friendly’, after the positive outcome the updated belief state coincides with the environmentally friendly belief state $|F\rangle$ (pink arrow).

13 Cognitive psychologists have discussed many key reasons for using quantum probability theory
 14 within cognitive modelling (Busemeyer et al., 2011), with many of these reasons also being trans-
 15 ferable and relevant within travel behaviour modelling. Firstly, a belief state is most often initially
 16 ‘indefinite’; it may either have some underlying preference in favour of an alternative or it may
 17 express uniform indifference with respect to the alternatives. This may come about due to dis-
 18 torted processing or lack of proper informative input. Furthermore, the final belief state is also
 19 in many instances *created* rather than just *recorded* by an effort to measure it. For example, a
 20 decision-maker might only start considering how environmentally friendly they are after they have
 21 been asked (or reminded) about how environmentally friendly they are (White et al., 2014). For
 22 this reason, it is often seen as essential that surveys including both choice tasks and attitudinal

1 questions require the respondent to complete the choice tasks first if the researcher wishes to avoid
2 bias in the choice task (Ben-Akiva et al., 2019). However, conversely, a decision-maker may try
3 to ‘justify’ their choices with their responses to the attitudinal questions (Cunha-e Sá et al., 2012).
4 Consequently, it is difficult to measure a decision-maker’s ‘true’ attitudes, opinions and preference
5 without some form of bias. It is easy to see how this relates to issues for choice modellers with, for
6 example, analysts often having concerns about the biases or truthfulness within stated preference
7 data (Mahieu et al., 2016).

8 Secondly, psychologists have put forward the argument that cognition behaves like a rip-
9 pling wave pattern rather than a classical particle trajectory (Trueblood and Busemeyer, 2012). A
10 decision-maker might consider the advantages of getting the train but then also consider the advan-
11 tages of driving. Indeed, many models developed in mathematical psychology assume preferences
12 for alternatives that update stochastically (Busemeyer and Townsend, 1993; Krajbich et al., 2012).
13 Under quantum probability theory, preference over time ‘behaves like a wave’ and consequently
14 exhibits interference patterns and fluctuates over time. It is only when a decision-maker makes
15 up their mind and makes a decision that their preference exists as some measurable definite state.
16 Before an action or choice is made, an observer does not know for sure what the decision-maker
17 will do. There are many preference states within travel behaviour that could similarly be described
18 as ‘wave-like’, such as anticipating merging onto a new lane when driving, changing travel mode
19 when the weather worsens, or choosing which route to take depending on traffic conditions.

20 One of the most crucial quantum concepts, however, is the idea of interferences, as e.g. change
21 caused by nudges (such as the previous example of being asked about the environment whilst in the
22 process of making a mode choice). After the development of quantum physics to explain ordering
23 effects of observed variables (Birkhoff and Von Neumann, 1936), a wide range of quantum mod-
24 els, often based on the idea of quantum interference, have been put forward in cognitive psychol-
25 ogy (Bruza et al., 2015). These include a quantum model to explain ordering effects (Trueblood
26 and Busemeyer, 2011), a quantum similarity model (Pothos et al., 2013), a quantum judgement
27 model (Busemeyer et al., 2011) and the disjunction effect in the Prisoner’s Dilemma (Moreira and
28 Wichert, 2016) and in the two-stage gamble paradigm (Broekaert et al., 2020). These models per-
29 form a similar function to choice models that include state dependence, where a number of different
30 models (Seetharaman, 2003) have been applied to capture the temporal correlation of choices over
31 time. Furthermore, should measurement data for both attitude and choice be provided, a higher
32 dimensional representation could be built. Such models have been presented in the literature and
33 have been applied in various contexts; e.g. for choice and confidence level (Kvam et al., 2015),
34 for choice and categorisation (Busemeyer et al., 2009) and choice, confidence and response time
35 (Busemeyer et al., 2006; Kempe, 2003). Given the success of quantum models at explaining or-
36 dering effects within cognitive psychology, there is ample scope for quantum logic and quantum
37 ideas within travel behaviour modelling and choice modelling in general.

38 **2.2. Choice making under quantum probability theory**

39 More formally, under quantum probability theory, a measurement (or choice scenario), X , can
40 be related geometrically to a subspace L_x in a multidimensional complex-valued Hilbert³ space

³A Hilbert space is a vector space over the set of real or complex numbers \mathbb{C} , (see e.g. Aerts and Gabora 2005). It is the more general form of a Euclidean space, extended to allow for complex numbers and defined over multiple (possibly infinite) dimensions and it is complete; i.e. a space for which convergent sums of vectors are again elements of the vector space. For the work in this paper, our Hilbert space is n -dimensional, where n is the number of choice

1 (Trueblood et al., 2014b). For each measurement, a number of discrete projection ‘events’ are
 2 possible. These projection events, if mutually exclusive, are related to orthonormal vectors⁴ in
 3 subspace L_x , which are denoted $|x_1\rangle$, $|x_2\rangle$, ... $|x_J\rangle$ (with J the number of alternatives). For these
 4 vectors, we use ‘bra-ket’ notation in keeping with the standard notation used in quantum mechanics
 5 and quantum cognition (c.f. Trueblood and Busemeyer 2011). Under bra-ket notation, a column
 6 vector in a Hilbert space is represented by a ‘ket’ vector, $|\cdot\rangle$, with the corresponding row vector
 7 (with each element being complex conjugated) a ‘bra’ vector, $\langle\cdot|$ (see e.g. Yu and Jayakrishnan
 8 2018). This bra-ket convention simplifies the expression of the inproduct of two states, in particular
 9 the squared norm of a complex-valued vector $|Z\rangle$ is then given by the real $\langle Z|Z\rangle$.

10 These orthonormal vectors, $|x_i\rangle$, then form a basis for the subspace L_x . Consequently, the
 11 Hilbert space for a choice task with J alternatives can be represented by a J -dimensional space. This
 12 means that for a choice set where there are three alternatives, the Hilbert space is a 3-dimensional
 13 space (illustrated in Figure 4).

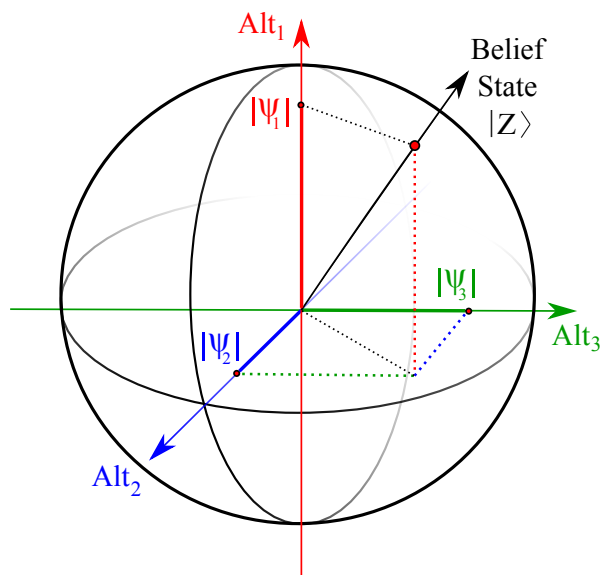


FIGURE 4 : Schematic representation of the belief state in the geometric quantum-like model for a three-choice paradigm $\{\text{‘Alt}_1\}$, ‘Alt₂’, ‘Alt₃’ $\}$ on the unit sphere (see Equation 2). The squared modulus of the amplitude obtained by projection on the axes for each alternative produces the respective probability for that choice $p(\text{Alt}_j) = |\psi_j|^2$.

14 **A basic choice.** Under quantum probability theory, a decision-maker has some ‘belief state’ re-
 15 garding their preferences over alternatives, which itself is probabilistic (in that a decision-maker
 16 inherently has some level of certainty over their preferences and opinions) and is denoted $|z\rangle$,
 17 which can be represented by a vector of unit length (see Figure 4). When a decision-maker makes
 18 a choice, their state goes from ‘indefinite’ to ‘definite’, by projecting onto the vector represent-
 19 ing the chosen alternative. This means that for each alternative Alt_j , with subspace L_{x_j} there is
 20 a corresponding projection operator P_{x_j} - formally $P_{x_j} = |x_j\rangle\langle x_j|$ - to project $|z\rangle$ onto the vector
 21 $|x_j\rangle$.

alternatives in a given choice task.

⁴More generally these can have more than one dimension, hence orthogonal subspaces should then be used.

1 The choice probability, $Pr[j]$, for a specific alternative Alt_j is given by the modulus square of
 2 the amplitude for that alternative appearing in the decision-maker's belief state;⁵

$$Pr[j] = |P_{x_j} |z\rangle|^2 = |\langle z|x_j\rangle|^2 = |\psi_j|^2. \quad (1)$$

3 Since we assume the presented alternatives exhaust all possible choices and each alternative is
 4 represented by an orthonormal vector (or set of such vectors), the belief state vector must be of
 5 unit length:

$$\sum_{j=1}^J |\psi_j|^2 = 1, \quad (2)$$

6 A visual check of this fact appears in Figure 4. The lengths of the three projections can be visu-
 7 alised as the three sides of the cuboid in 3-dimensional space in which Pythagoras' theorem can be
 8 applied sequentially.

9 **A sequence of choices.** If a decision-maker makes a second choice across a different set of
 10 alternatives, this choice may be influenced by the first. Quantum probability theory captures this
 11 influence by representing the two measurement events by two separate subspaces within the Hilbert
 12 space, L_x and L_y . Each subspace is separately defined by a set of orthonormal vectors representing
 13 the alternatives in each measurement event. This means that L_x is spanned by $|x_1\rangle, |x_2\rangle, \dots |x_J\rangle$
 14 and L_y is spanned by $|y_1\rangle, |y_2\rangle, \dots |y_K\rangle$, where there are J alternatives for choice scenario X and
 15 K alternatives for scenario Y (while it must be assured that both scenarios span the same Hilbert
 16 space).

17 Revisiting the example presented in Figure 3, a decision-maker might initially be making a
 18 choice between commuting by car or train. Under quantum probability theory, the decision-maker
 19 has some initial belief state, informed by past experience, regarding whether they will choose car
 20 or train. In this measurement event, all possible states are spanned by the basis vectors $|x_{car}\rangle,$
 21 $|x_{train}\rangle$. The closer the vector representing the decision-maker's state is to the vector representing
 22 an alternative, the more likely it is for that alternative to be chosen. However, the decision-maker
 23 could first be asked a different question (Y) about whether they consider themselves to be environ-
 24 mentally friendly or not. In the 'change of perspective' approach of quantum probability theory,
 25 the initial belief state does not change under the new perspective under question Y , but the refer-
 26 ence frame does. This means that the probabilities for alternatives being chosen in question Y are
 27 different from the probabilities for alternatives being chosen in question X because the choice in
 28 question Y is represented by a different set of basis vectors, $|y_{env-friendly}\rangle, |y_{env-unfriendly}\rangle$. Con-
 29 sequently, if the decision-maker makes the choice 'I am environmentally friendly', their belief state
 30 moves through the Hilbert space, projected onto the environmentally friendly vector, $|y_{env-friendly}\rangle$
 31 (see Figure 3). This means that their new belief state is the vector $|y_{env-friendly}\rangle$ itself. Hence, by
 32 making choice in question Y first, the original choice X between car and train is made from a
 33 different belief state.

34 Crucially, by moving their belief state - through what we call a 'quantum rotation' - the size of

⁵Using the bra-ket notation, one can easily see:

$$|P_{x_j} |z\rangle|^2 = ||x_j\rangle\langle x_j|z\rangle|^2 = \langle z|x_j\rangle\langle x_j|x_j\rangle\langle x_j|z\rangle = \langle z|x_j\rangle\langle x_j|z\rangle = |\langle z|x_j\rangle|^2$$

1 the projected amplitudes onto the vectors for train and for car have changed.⁶ As a result, in this
 2 example, the decision-maker is more likely to choose to commute by train if they first decide that
 3 they are environmentally friendly. This is graphically represented in Figure 3, where the size of the
 4 projected amplitude onto the basis vector representing train being chosen has increased, resulting
 5 in an increased probability of choosing train.

6 3. BUILDING A CHOICE MODEL FROM QUANTUM PROBABILITY THEORY

7 Whilst Lipovetsky (2018) has applied quantum models to consumer recall tasks with multiple
 8 alternatives defined on multiple attributes, quantum probability has not ever been applied to multi-
 9 alternative, multi-attribute choice scenarios (as far as the authors are aware). In this section, we
 10 look at how we can use ideas from quantum probability within a choice model. We do this by
 11 first considering what the requirements are for a quantum choice model. Next, we formally define
 12 our two alternative quantum-like models, one based on an amplitude approach and the other on a
 13 Hamiltonian approach. We then consider how similar or related choice tasks could be mathemati-
 14 cally explained by a ‘quantum rotation’. Finally, we discuss a number of different value functions
 15 that we implement within both standard choice models and our new quantum choice models.

16 For our choice model to use quantum probability theory, we need to define a method for con-
 17 structing an indefinite state vector. If this state vector is of unit length and we take projections
 18 from it to a set of orthonormal basis vectors (with one vector for each discrete alternative), then
 19 the sum of the squared length -more precisely the amplitude- of these projections will equal one.
 20 Consequently, for each alternative, we need to find the amplitude of the projection, as the square of
 21 this ‘length’ equals the probability with which the alternative is chosen (see Figure 4). This means
 22 that we must first consider how best to represent the state vector, $|z\rangle$.

23 If, for example, we imagine that we are making a route choice between three alternatives, the
 24 development of a state could be represented by Figure 5. When the decision-maker considers
 25 factors favouring alternative 1, the state vector extends in the direction of the vector representing
 26 alternative 1 (and hence increasing the amplitude of the projection onto alternative 1). Similarly,
 27 the decision-maker may consider factors that favour alternatives 2 and 3, resulting in the state vec-
 28 tor extending in the direction of the vector for alternative 2 or 3. At some point, the decision-maker
 29 reaches some eventual state and makes the actual (probabilistic) choice.⁷ To generate this state, we
 30 need to know the relative importance of the attributes. This means that one option is to calculate
 31 ‘value functions’ for each alternative. However, if we write the value functions, $V_j = \beta'x_j$, where
 32 β is a vector of coefficients and x_j is a vector of observed variables relating to alternative j, then
 33 V_j can be positive or negative. As the probability of an alternative is the squared ‘length’ of the
 34 projection from the state vector onto the vector for the alternative, positive and negative values
 35 would lead to the same result. This means that care is required when defining how the relative
 36 values of the attributes impact the probability amplitudes.

37 A further requirement for quantum models is some method for capturing underlying prefer-
 38 ences towards an alternative. In the representation for the development of an informed state in
 39 Figure 5, this simply means having some initial state that is still uninformed by the attributes, but

⁶Two choices that require a different set of basis vectors are known as ‘incompatible’. If the choices are in fact compatible and can be represented by the same set of basis vectors, then the order in which the choices are made has no impact on the probabilities of each alternative being chosen. Consequently, quantum probability collapses back into classical probability (Hughes, 1992).

⁷Note that this choice remains probabilistic unless the decision-maker is 100% certain about their choice.

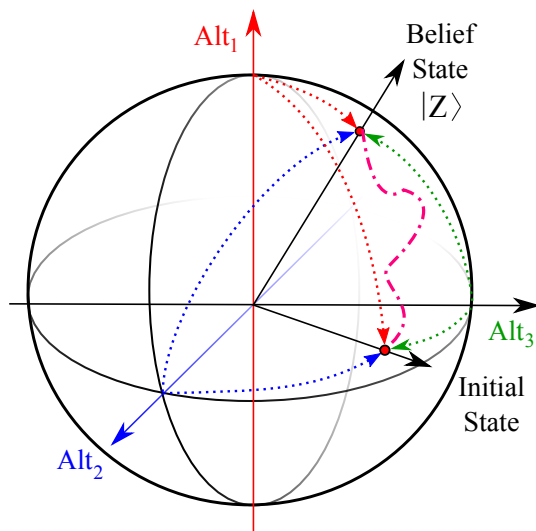


FIGURE 5 : Schematic representation of the development of an informed belief state. The quantum-like dynamical approach lets the ‘uninformed’ - or possibly biased - initial state evolve to an informed state which leads to the final belief state underlying the probabilistic decision. In the amplitude model this transformation is caused by the subjective utility comparisons immediately in the vector components, while in the Hamiltonian model these utility differences drive the Hamiltonian operator of change over time.

1 is only based on underlying preferences towards an alternative. Thus, the initial state should be
 2 defined on some parameters that act equivalently to attribute specific constants. Then subsequently,
 3 from this initial state, the evolution happens when the decision-maker considers the attributes of
 4 the alternatives.

5 3.1. The quantum-amplitude model

6 Similar to geometric quantum models, the quantum-amplitude model is directed at implementing
 7 a specific functionality of the amplitude components of the belief-action state themselves. The
 8 innovative approach is to implement value functions for the attributes of the alternatives in the
 9 amplitudes. This approach will show an increased optimisation performance since the supporting
 10 factors for each of the alternatives are directly expressed in the choice probabilities - through the
 11 respective amplitudes.⁸

12 In geometric approaches, belief states are mostly real-valued vectors of the n -dimensional Eu-
 13 clidean space, e.g. Pothos et al. (2013); van Rijsbergen (2004), or points on the n -dimensional
 14 hypersphere.⁹

15 In the ‘quantum-amplitude’ approach, we consider the full potential of complex-valued belief

⁸This is in contrast with the Hamiltonian model in which the value functions are implemented in the Hamiltonian components which drive the decision process by progressing the belief state over time and which thus only indirectly produce the choice probabilities.

⁹These belief-state vectors can then be expressed either using generalised spherical coordinates (e.g Lipovetsky (2018); Blumenson (1960)):

$$\begin{aligned} \psi_1 &= \cos \phi_1, & \psi_2 &= \sin \phi_1 \cos \phi_2, & \psi_3 &= \sin \phi_1 \sin \phi_2 \cos \phi_3, & \dots \\ \psi_{n-1} &= \sin \phi_1 \sin \phi_2 \dots \sin \phi_{n-1} \cos \phi_n, & \psi_n &= \sin \phi_1 \sin \phi_2 \dots \sin \phi_{n-1} \sin \phi_n \end{aligned}$$

1 amplitudes to *directly estimate the choice probabilities*. Thus, rather than *evolving* an initial state
 2 to a final belief-state vector, in this model we specifically optimise the proper complex amplitudes
 3 of the final belief state itself.

4 For each individual, alternative i in a given choice task has an amplitude, ψ_i , which is estimated
 5 as the sum of subjective differences between it and other alternatives j :

$$\psi_i = \left(\delta_i + \sum_{i \neq j} \Delta_{ij} \right) / \sqrt{\mathcal{N}}, \quad (3)$$

6 where Δ_{ij} is the subjective difference between alternatives i and j (see Section 3.4 for details on the
 7 four different value functions that we test to represent this subjective difference) and δ_i is a constant
 8 for alternative i which implements the mean impact in the sample of any factors omitted from the
 9 specification of the value function for that alternative. This can cover both omitted attributes as well
 10 as underlying preferences for specific alternatives. These constants will only take a value of zero
 11 if, in the situation of all included explanatory variables taking the same value for the alternatives,
 12 the probabilities will be equal. Both Δ_{ij} and δ_i depend on the individual respondent and the task at
 13 hand. The normalisation factor (which ensures Equation 2 holds), $\sqrt{\mathcal{N}}$, is obtained from the sum
 14 of the squared moduli:

$$\mathcal{N} = \sum_i \left| \delta_i + \sum_{i \neq j} \Delta_{ij} \right|^2. \quad (4)$$

15 Whereas adding the same constant to the utility of every alternative does not have an impact in
 16 random utility models, the multiplication of the amplitudes by the same constant does not impact
 17 the choice probabilities of alternatives under a quantum system (see Equation 2). Consequently,
 18 we can have J parameters to capture the underlying preference towards the J alternatives. The
 19 greater the magnitude of these constants, δ_i , relative to the magnitude of the differences, Δ_{ij} ,
 20 the less deterministic the choices become. Note that from a mathematical point of view we can
 21 equivalently estimate the corresponding probabilities, instead of the amplitudes Equation (3), in
 22 the model parameter optimisation process (Section 5). Finally, we note that the amplitude model is
 23 more general than the cosine similarity model in that it also allows for complex-valued functional
 24 expressions, Δ_{ij} , of subjective attribute differences of the alternatives (see section 5.2).

25 3.2. The quantum-Hamiltonian model

26 In the search for an adequate dynamical approach to the decision process, quantum *dynamical* el-
 27 ements have proven effective in covering experimental choice paradigms involving ordering and
 28 contextuality (Aerts et al., 1999; Busemeyer et al., 2006; Atmanspacher and Filk, 2010; Fuss and
 29 Navarro, 2013; Martínez-Martínez, 2014; Asano et al., 2015; Kvam et al., 2015; Broekaert et al.,
 30 2017, 2020; Bagarello, 2019). An introductory treatment of this quantum dynamical approach in
 31 decision making can be found in Busemeyer and Bruza (2012)'s handbook. At the core of this

or by using similarity angles (Pothos et al., 2013) as given by (see Figure 2);

$$\psi_1 = \cos \theta_1, \dots, \psi_i = \cos \theta_i, \dots, \psi_n = \cos \theta_n$$

in which the similarity cosines must satisfy state normalisation $\sum_{i=1}^n \cos^2 \theta_i = 1$.

1 approach is the operator which drives the change of a state vector in quantum theory; the *Hamiltonian*.¹⁰ In contrast to the quantum-amplitude model (see Section 3.1), the ‘quantum-Hamiltonian’
 2 model thus implements the behavioural decision process as an evolution of the belief state over
 3 time. In this dynamical choice model the stochastic process underlying the change of a partic-
 4 ipant’s belief state over time will now be driven through a Hamiltonian which implements the
 5 comparison of the attributes of the alternatives. More specifically, the Hamiltonian operator H
 6 controls the change of the state vector according to the dynamics of the Schrödinger equation:
 7

$$-i\frac{d}{dt}\Psi = H\Psi, \quad (5)$$

8 where we have assumed dimensionless expressions for time and ‘energy’.¹¹ The only formal
 9 requirement on the Hamiltonian is Hermiticity, $H^\dagger = H$, i.e. the transpose conjugate of matrix H
 10 returns H itself. This property assures that the time evolution will conserve the normalisation of
 11 the belief state at all times and thus ensure that the choice probabilities across the alternatives add
 12 up to 1.

13 The driving factors of the decision task are formally integrated in the Hamiltonian according
 14 to a parametrised Hadamard gate (Busemeyer and Bruza, 2012; Broekaert et al., 2017)

$$H = \begin{pmatrix} h_{11} & \delta_{12} + \Delta_{12} \\ \delta_{12}^* + \Delta_{12}^* & -1 \end{pmatrix}, \quad (6)$$

15 where * indicates the complex conjugate. It should be remarked however that factors in the off-
 16 diagonal elements of the Hamiltonian serve a different dynamical function than in the amplitude
 17 model (Equation 3). In the Hamiltonian model, the drivers embody pairwise symmetric compar-
 18 isons of attributes of two alternatives which dynamically compete with each other. For more than
 19 two alternatives, we can estimate additional diagonal elements, h_{jj} and each pairwise comparison
 20 of alternatives is implemented in a separate parallel process by allocating the drivers to the proper
 21 matrix positions;¹²

$$h_{ij} = \delta_{ij} + \Delta_{ij}. \quad (i \neq j) \quad (7)$$

22 In the amplitude model, on the other hand, all pairwise attribute comparisons are immediately
 23 summed into the resulting probability amplitude. The driving factors, $\{\delta, \Delta\}$, therefore serve a
 24 very different modelling purpose in the two quantum approaches.

25 The changed belief state at each moment of time is the solution of the Schrödinger equation
 26 (see equation 5). This solution can be easily expressed by calculating the propagator:

$$U(t) = e^{-iHt}, \quad (8)$$

¹⁰A formally very similar dynamic model is provided by continuous-time Markov chain theory in which the operator of change is the transition rate matrix or ‘intensity’ matrix (see e.g. Busemeyer and Bruza 2012).

¹¹In quantum-like modelling in decision making, Planck’s constant is set equal to 1 as a standard. This essentially introduces a scale factor to ‘time’ in the decision process. The Hamiltonian is the generator of change over time but is further devoid of energy connotation.

¹²The Hamiltonian model can be extended to encompass non-symmetric comparison of attributes by doubling the dimension of the Hilbert space. The belief state for each alternative then consists of a two-dimensional subspace.

1 and applying it to the initial belief state:

$$\Psi(t) = U(t)\Psi(0). \quad (9)$$

2 In the Hamiltonian model, the unitary time-propagator thus evolves the uninformed - and in gen-
3 eral, unbiased - initial belief state $\Psi(0)$ into the evolving informed belief state $\Psi(t)$

$$\Psi(0) = \begin{pmatrix} 1/\sqrt{2} \\ 1/\sqrt{2} \end{pmatrix} \longrightarrow \Psi(t) = \begin{pmatrix} \psi_1(t) \\ \psi_2(t) \end{pmatrix}. \quad (10)$$

4 Like in the general quantum-like approach, to obtain the choice probability for a particular alter-
5 native in the experimental paradigm, the corresponding subspace projector M_j should be applied
6 and its outcome norm-squared; $\|M_j\Psi(t)\|^2$. One more crucial formal element in the Hamiltonian
7 formalism for a decision process is thus the *time of measurement*. Since the datasets we cover in
8 our present study do not include reaction times, we can fix this time to $\pi/2$ in accordance with
9 standard time-scaling procedures (Busemeyer and Bruza, 2012).¹³

10 3.3. Quantum rotations

11 In Section 2.1 and Figure 3, we demonstrated how a ‘change of perspective’ could be accomplished
12 by a projection onto a system with rotated axes representing the new context of the decision. In
13 an equivalent active implementation, this change of perspective can be incurred by applying a
14 rotation operation on the belief state itself (whereas a passive implementation would rotate the basis
15 vectors). For the simplest example with two alternatives, this rotation occurs in a 2-dimensional
16 Hilbert space. The quantum generators of such rotations are the Pauli matrices, e.g. (Feynman
17 et al. 1965, Ch.11);

$$\sigma_x = \begin{pmatrix} 0 & 1 \\ 1 & 0 \end{pmatrix}, \quad \sigma_y = \begin{pmatrix} 0 & -i \\ i & 0 \end{pmatrix}, \quad \sigma_z = \begin{pmatrix} 1 & 0 \\ 0 & -1 \end{pmatrix}. \quad (11)$$

18 The rotation operator, R , itself - about axis $\mathbf{n} = (n_x, n_y, n_z)$ and over angle ϑ - is then given by;¹⁴

$$R = e^{-i\vartheta\mathbf{n}\cdot\boldsymbol{\sigma}}, \quad (12)$$

19 where $\mathbf{n} \cdot \boldsymbol{\sigma}$ gives some combination of the Pauli factors, with the restriction that $|\mathbf{n}| = 1$. These
20 rotation operations will be applicable in two of the covered experimental paradigms in our present
21 study (see Section 5).

22 3.4. Value functions: linear difference, asymmetric decay, soft plus

23 As well as the use of different ‘error structures’ provided by the different models, we can also
24 improve our models through the use of non-linear value functions to translate objective differences

¹³Note that a more elaborate quantum model, with intermediate and iterated response/no-response reductions, is required to handle response times (Busemeyer et al., 2006; Kempe, 2003)

¹⁴Using the equivalence

$$e^{-i\vartheta\mathbf{n}\cdot\boldsymbol{\sigma}} = \mathbf{1} \cos \vartheta - i\mathbf{n} \cdot \boldsymbol{\sigma} \sin \vartheta,$$

it is easily verified that for $n_y = 1$, one retrieves the classical expression for a rotation matrix in the real plane, e.g. (Busemeyer and Bruza, 2012; Broekaert et al., 2017).

1 into subjective ones. In this paper, we test four different value functions across our logit and
2 quantum-like models.

3 **Linear Difference function (LD).** The first value function we use simply calculates the relative
4 importance of the linear differences in attributes. Thus, for respondent n in choice task t , we define
5 the subjective difference between alternatives i and j as:

$$\Delta_{ij} = \sum_{k=1}^K \beta_k \cdot (x_{ik} - x_{jk}), \quad (\text{LD}) \quad (13)$$

6 where $k = 1, \dots, K$ is an index across attributes, β_k a coefficient for the relative importance of
7 attribute k and x_{ik} and x_{jk} are the values for alternatives i and j for attribute k .

8 **Asymmetric Decaying Linear Difference function (ADLD).** The second value function we
9 test is based on the use of drift rate functions from the multi-attribute linear ballistic accumulator
10 model (Trueblood et al., 2014a). The linear ballistic accumulator (LBA), was originally designed
11 within mathematical psychology, and is a model designed to capture both choices and response
12 times (Brown and Heathcote, 2008). In this approach, a decision-maker starts with a random
13 amount of evidence for each alternative. The evidence for each alternative then grows linearly
14 according to a set of drift rates (with one rate for each alternative). The first to reach some thresh-
15 old is then the chosen alternative. This model was then adjusted for alternatives with multiple
16 attributes (MLBA) and has been used successfully to explain choices between ratings for eyewit-
17 ness testimony (Trueblood et al., 2014a), consumer and perceptual choices (Turner et al., 2018) and
18 gambling and accommodation choices (Cohen et al., 2017). In the approach for multiple attributes,
19 the drift rates are generated from a normal distribution where the mean drift rates are a function
20 of the attributes of the alternatives. The non-linearity in the specification for the drift rates allows
21 for the explanation of the similarity, attraction and compromise effects. Notably, work such as
22 Guevara and Fukushi (2016) and Hancock et al. (2018) demonstrate that models that can account
23 for these context effects can be effective for understanding travel behaviour. The corresponding
24 non-linear expression for the drift rate is the second value function we test in this paper:

$$\Delta_{ij} = \sum_{k=1}^K w_{x_{ijk}} \cdot \beta_k \cdot (x_{ik} - x_{jk}), \quad (\text{ADLD}) \quad (14)$$

25 where $w_{x_{ijk}}$ is a similarity weighting and β_k , x_{ik} and x_{jk} are defined as before. Whilst similar in
26 appearance to regret functions (see Equation 16), this function, rather than using a logarithm, uses
27 similarity weightings. These are defined such that they are an exponentially decaying function of
28 distance (dropping the indices for individual and task):

$$w_{x_{ijk}} = \exp\left(-(\lambda_1 \cdot [x_{ik} \geq x_{jk}] + \lambda_2 [x_{ik} < x_{jk}]) \cdot \beta_k \cdot |x_{ik} - x_{jk}|\right), \quad (15)$$

29 where the square brackets convert to 0 or 1 according to the conditional test whether attribute value
30 k is larger in Alt_i than in Alt_j , or vice versa. Under MLBA, two different values, λ_1 and λ_2 , are
31 used to capture Tversky (1977)'s findings that the subjective similarity between A and B and the
32 subjective similarity between B and A may not be equal. Given that differences between losses and
33 gains have regularly been shown to be important in a transport context (Hess et al., 2008; Masiero
34 and Hensher, 2010; Stathopoulos and Hess, 2012), this is a useful feature for this quantum model

1 as well. Both λ values should be greater than zero to ensure that attributes that are more similar
 2 have a higher similarity value $w_{x_{ijk}}$. This results in weights that are between 0 and 1.¹⁵ Whilst
 3 MLBA models typically use just a single pair of λ parameters, another option is to have pairs that
 4 are specific to each attribute (i.e. λ_{1k} and λ_{2k}), though this would of course lead to a large increase
 5 in the number of estimated parameters if there is a large number of attributes.

6 **Softplus function (S+)**. The third value function we test is derived from ‘softplus’ functions,
 7 which are used for the activation of a node depending on inputs in a neural network (Hahnloser
 8 et al., 2000) and are frequently implemented within machine learning (Dugas et al., 2001; Nair and
 9 Hinton, 2010; Zheng et al., 2015). This function is better known in choice modelling for their use
 10 within regret functions from random regret minimisation (RRM). The deterministic regret (Chorus,
 11 2010) for the difference between two alternatives i and j is:

$$\Delta_{ij} = \sum_{k=1}^K \ln(1 + e^{\beta_k(x_{jk} - x_{ik})}), \quad (\text{S+}) \quad (16)$$

12 with β_k , x_{ik} and x_{jk} defined as before.

13 **μ -RRM function (μ -RRM)**. The final value function we use is based on μ -RRM (van Cra-
 14 nenburgh et al., 2015), which is designed to estimate the ‘profundity of regret’. It is defined as:

$$\Delta_{ij} = \mu \cdot \sum_{k=1}^K \ln(1 + e^{\frac{\beta_k}{\mu}(x_{jk} - x_{ik})}), \quad (\mu - \text{RRM}) \quad (17)$$

15 where μ is a parameter that results in the function collapsing to the LD function (Equation 13) if it
 16 is arbitrarily large, and to the S+ function (Equation 16) if it is close to a value of 1.

17 The use of the four different value functions for Δ_{ij} together with Equations (A1, A2), in the
 18 Appendix, of the Logit approach, thus correspond to a multinomial logit (MNL), a contextual
 19 utility model and random regret minimisation models (RRM, μ -RRM), respectively. We compare
 20 these base models against all of these value functions combined with quantum choice models in
 21 Section 5.1.

22 4. DATA FOR EMPIRICAL EXAMPLES

23 In this paper, we test our different specifications of quantum models on a number of travel be-
 24 haviour datasets, which we now describe in turn.

25 4.1. Swiss value of time dataset

26 The first dataset we use comes from the Swiss value of time study (Axhausen et al., 2008), where
 27 389 participants each make 9 binary route choice tasks. The two alternatives are described by travel
 28 cost (CHF), travel time (minutes), headway (minutes) and the number of interchanges required
 29 to complete the trip. This is a basic route choice dataset, without the possibility of testing for
 30 interference effects, i.e. an absence of conditions that are specifically suitable for quantum models.
 31 We include this ‘basic’ dataset to test how our quantum models perform under basic settings (i.e.
 32 when there is no need for a ‘quantum rotation’). This allows us to test whether the underlying
 33 structure for the quantum models is effective for modelling travel behaviour.

¹⁵Note that we adjust the drift rate specification and the weighting functions from the standard specification in Trueblood et al. (2014a) to include weights (β_k) for the relative importance of different attributes.

1 **4.2. UK value of time dataset**

2 The second dataset that we use in this paper comes from the most recent value of travel time study
 3 conducted in the UK (Batley et al., 2017). This dataset comprises of 15,045 choices between two
 4 balanced alternatives, one of which is cheaper and the other faster (SP1 in Batley et al. 2017). This
 5 second dataset allows us to consider quantum rotations to understand the impact of a change in the
 6 position of the alternatives or the attributes. In the lay-out of the UK value of time paradigm, two
 7 travel alternatives are juxtaposed and are ordered according to two variations;

8 **Time on top:** 1) the shorter time but more expensive alternative on the left of the page and thus
 9 the longer time but cheaper alternative on the right ‘t/C-T/c’, and 2) the longer time alternative on
 10 the left of the page and thus the shorter time on the right ‘T/c-t/C’.

11 Different respondents received the same alternatives and orders, but with inverted ordering of the
 12 textual formulation (‘phrasing’) of the time and cost of the alternative. With these adapted formu-
 13 lations of the options, the two alternatives were again presented in both relative positions.

14 **Cost on top:** 1) the configuration with shorter time alternative on the left ‘C/t-c/T’, and 2) the
 15 configuration with longer time alternative on the left ‘c/T-C/t’.

16 The aggregated respondent preferences given in Table 1, show the option order variation¹⁶ to have
 17 a significant influence on choice.¹⁷

TABLE 1 : Observed choice share for alternative 1 in UK-Context paradigm

	Option Order 1	Option Order 2
Textual Order 1	0.495	0.474
Textual Order 2	0.517	0.473

18 Initial tests suggest that the option order shows a bias effect on the choices made by the respon-
 19 dents, with $\chi^2(1, N = 15045) = 15.884, p = 6.735e - 5$. However, we see that the textual order
 20 does not, with $\chi^2(1, N = 15045) = 1.628, p = 0.280$. These effects cannot however be disentan-
 21 gled from the impacts of changes in attributes levels in choice tasks, as whilst a balanced design
 22 is used to create the choice tasks, the attribute levels are based on a reference trip, meaning that
 23 contextual effects can only be disentangled through the estimation of models jointly incorporating
 24 the impact of all attributes.

25 **4.3. UK best-worst dataset**

26 The third dataset uses the best-worst format, allowing us to test quantum rotations for their ability
 27 to capture both best and worst choices simultaneously. The best-worst dataset we use comes from
 28 a survey asking public transport commuters living in the UK to make a set of ten choices between
 29 three route alternatives in a stated preference survey. Each choice task involves an invariant refer-
 30 ence trip and two hypothetical alternatives. In each instance, the first alternative corresponded to
 31 the current respondent-specific conditions. The attributes of the two other alternatives are pivoted
 32 around the attributes of the status quo alternative, where the design process ensured that none of

¹⁶Note that $\text{Prob}(\text{Alt}_2) = 1 - \text{Prob}(\text{Alt}_1)$ in Table 1.

¹⁷Notice that order effects in quantum-like modelling have been covered previously for consecutive execution of tasks over time and in varied order of execution. In the current paradigm, the order effect relates to variations of visual presentation and phrasing ordering all in the same instance of time.

1 the three alternatives dominates. Each alternative is described by six attributes: travel time (in
 2 minutes), fare (£), rate of crowded trips, rate of delays (both out of 10 trips), the average length
 3 of delays (across delayed trips) and the provision of delay information service (which could be
 4 unavailable, available at a cost, or available for free). A total of 391 participants completed 10
 5 choice tasks. The participant’s task consists of choosing the best option out of the three presented
 6 alternatives, and the worst option out of the two remaining alternatives. As participants choose a
 7 best and a worst alternative in each choice task, we have a total of 7,820 choices. For full details
 8 of the dataset, readers should refer to [Stathopoulos and Hess \(2012\)](#). Crucially, in this best-worst
 9 choice data, a bias can be observed in the respondent choice shares, which are given in [Table 2](#),
 10 with respondents tending to choose alternatives 2 or 3 as their least favoured alternative more often
 11 than their current trip (alternative 1), $\chi^2(2, N = 7820) = 899.9, p < 2.2e - 16$.

TABLE 2 : Joint Choice Probabilities and marginals in UK-Best/Worst paradigm

	Alternative 1 worst	Alternative 2 worst	Alternative 3 worst	Sum
Alternative 1 best	•	0.198	0.149	0.347
Alternative 2 best	0.098	•	0.251	0.349
Alternative 3 best	0.058	0.246	•	0.303
Sum	0.156	0.444	0.400	1

12 5. EMPIRICAL APPLICATIONS

13 In this section, we describe the various empirical exercises conducted on the data described in
 14 [Section 4](#). We start with basic models, before increasing the complexity of the models. Finally,
 15 we consider out of sample validation for quantum rotations. For all models, we use R packages
 16 [maxLik \(Henningsen and Toomet, 2011\)](#) and [Apollo \(Hess and Palma, 2019\)](#) for estimation of the
 17 log-likelihood functions.

18 5.1. Basic models: logit, DFT, q-Hamilton, q-amplitude.

19 For the first test of our quantum models, we use all three datasets (Swiss, UK-Context and UK-
 20 Best/Worst). At this point, we do not yet consider quantum rotations, simply focussing on com-
 21 paring the different modelling approaches as well as testing the impact of using different value
 22 functions. Whilst these value functions can incorporate real and imaginary parts for the quantum
 23 choice models, we test real-only value functions in this section, with comparisons using imaginary
 24 parts in [Section 5.2](#). For all three datasets, we compare the quantum models against multinomial
 25 logit (MNL), random regret minimisation (RRM), $\mu - RRM$ and a contextual utility model with
 26 ADLD value functions (from MLBA theory, as defined in [Section 3.4](#)). All of these models have
 27 the assumption of no error correlation across choices (thus all choices are treated as being inde-
 28 pendent from each other, with no correlation assumed between sequential choices), as at this point,
 29 we wish to test the impact of simply changing the value function or changing from a classical
 30 error structure (which assumes extreme value errors) to quantum choice models.¹⁸ We also test

¹⁸We report robust standard errors throughout as the computation of the covariance matrix then also accounts for the repeated choice nature of the data, which generally results in an upwards correction of standard errors (cf. [Daly and Hess \(2010\)](#)).

1 our models against Decision Field Theory (DFT), which was demonstrated to outperform standard
 2 choice models in our previous research (Hancock et al., 2018). DFT is a dynamic stochastic choice
 3 model under which the preferences for different alternatives update over time within the context
 4 of a single choice. For a full description of the model, please refer to the Appendix. We first
 5 look at specific considerations for the best-worst data, before discussing model specification more
 6 generally, and then presenting the results.

7 5.1.1. Best-worst data modelling methodology

8 For the best-worst data, we at this point make the basic assumption that best is the opposite of
 9 worst. In a utility context, it is common practice to assume symmetry between best and worst,¹⁹
 10 such that:

$$U(\text{Alt}_{i \text{ worst}}) = -U(\text{Alt}_{i \text{ best}}). \quad (18)$$

11 For quantum models, however, this translation is not as simple for amplitudes. This is a conse-
 12 quence of using the squared amplitudes to calculate the probability of choice of alternatives (see
 13 Equation 1), when negative amplitudes for each projection will result in the same probabilities for
 14 each alternative as the corresponding positive projections. In the case of only three alternatives (a
 15 regular setting for many surveys), there however exists a simple transformation. Given that there
 16 are two alternatives left after choosing the most preferred, the probability of picking one alterna-
 17 tive as the second best (or second most preferred) equals the probability of picking the other as the
 18 worst. Consequently, given alternatives i and j , we can simply define the amplitudes for alternative
 19 i being the worst as:

$$|\psi_{\text{worst}_i}| = |\psi_{\text{best}_j}|, \quad (\text{basic inversion}) \quad (19)$$

20 which we define as a ‘basic inversion’ as it corresponds to the utility model in Equation 18, in that
 21 the factors that determine best and worst choice are identical.

22 For all models, the decision process of the best-worst choice task can be analysed as a progres-
 23 sion of a single encompassing process in which valuations of the first stage of choosing the best
 24 alternative are carried over into the subsequent process of choosing the worst alternative. On the
 25 other hand, these two stages of choice making can be considered to occur independently of each
 26 other without carry-over of previous outcomes. Mathematically, this means that in a ‘continued
 27 deliberation’ approach, utilities or amplitudes are generated using the appropriate value function
 28 to estimate the probability of each alternative being chosen as the best. Equations 18 and 19 are
 29 then used to generate the probability for the worst alternative directly, without a new evaluation
 30 of utilities or amplitudes. In an ‘independent’ evaluation approach, the utilities and amplitudes
 31 are re-evaluated for worst choice, where attribute differences between the alternative chosen as the
 32 best and the remaining alternatives are not included (thus, for example, under the amplitude model,
 33 Equation 3 would no longer have a summation, simply requiring Δ_{ij} where i and j are the only two
 34 remaining alternatives).

35 5.1.2. General points on model specification

36 For the models tested in this section, we have the following parameters:

¹⁹This is an oversimplification, with recent work demonstrating that an alternative is to use a scaling parameter, α , for the difference in scale between best and worst Hawkins et al. (2019). Alternatively, one can use a completely separate set of parameters for best choice compared to worst choice (Giergiczny et al., 2017), a point to which we return in Sections 5.3 and 5.4.

- 1 • **All models:** A relative importance parameter (β_k) for each attribute (4, 2 and 8 parameters
2 respectively for the Swiss, UK value of time and UK best-worst datasets.²⁰)
- 3 • **Utility models:** $J - 1$ alternative specific constants (1, 1 and 2 parameters respectively for
4 the Swiss, UK value of time and UK best-worst datasets).
- 5 • **DFT models:** $J - 1$ alternative specific constants (1, 1 and 2 parameters respectively for the
6 Swiss, UK value of time and UK best-worst datasets). All DFT models have 1 additional
7 estimated parameter for the number of preference updating steps, with the UK best-worst
8 model additionally having two feedback matrix parameters, ϕ_1 and ϕ_2 . These two parameters
9 were found to be insignificant for the Swiss and UK value of time datasets (in line with
10 previous results for datasets comprised of choices tasks with 2 alternatives, Hancock et al.
11 2020) and were therefore omitted. Note that as we use attribute scaling coefficients in our
12 DFT models (see Appendix), we fix the error $\sigma_\epsilon = 1$ for normalisation purposes.
- 13 • **Hamiltonian models:** 1 alternative pair constant for the Swiss and UK value of time datasets
14 and 3 for the UK best-worst dataset. We also have $J - 1$ Hamiltonian matrix diagonals (1, 1
15 and 2 parameters respectively for the Swiss, UK value of time and UK best-worst datasets).
16 Finally, the Hamiltonian models for UK best-worst models incorporating ‘independent de-
17 liberations’ has different Hamiltonian matrices for best and worst choice. For best choice, a
18 3x3 matrix is required, thus 2 parameters are required, whilst for worst choice, we require a
19 2x2 matrix, meaning that 1 additional parameter is required.
- 20 • **Amplitude models:** J alternative specific constants (2, 2 and 3 parameters respectively for
21 the Swiss, UK value of time and UK best-worst datasets).
- 22 • **ADLD value function:** 2 additional parameters for the utility model, λ_1 and λ_2 . For the
23 Hamiltonian model, we only estimate a single λ as we set $\lambda_1 = \lambda_2$ such that $\Delta_{ij} = \Delta_{ji}$ and
24 the Hamiltonian matrix remains Hermitian. DFT similarly requires $\Delta_{ij} = \Delta_{ji}$, thus only has
25 one λ estimated (See explanation of this in the Appendix). For the amplitude models, we
26 fix one λ parameter to a value of 1, as dividing λ by some value x and multiplying the
27 β parameters by x results in amplitudes that are also multiplied by x (hence normalisation
28 results in exactly the same probabilities and an overspecification if we do not fix a λ).
- 29 • **ADLDpA value function:** Has a set of lambdas for each attribute (‘ADLD per Attr.’). This
30 results in an insubstantial change in log-likelihood for the Swiss and UK best-worst datasets,
31 thus we only show the results for the UK value of time dataset. As this dataset has two
32 attributes, it has a total of 4 λ -parameters in the utility model, and 2 in the Hamiltonian and
33 DFT models (with the same restrictions applied from above).
- 34 • **μ -RRM value function:** 1 additional parameter, μ , which measures the profundity of regret.

²⁰Note that the UK best-worst dataset has choice alternatives with 6 attributes. The provision and cost of delay information service are treated separately, and we also have a ‘reliability’ index, which is the expected delay, defined as the interaction between the average time delay and the rate of delays, which was found to be significant in previous research (Stathopoulos and Hess, 2012).

1 5.1.3. Estimation results

2 The results for all of the basic models²¹ are given in Table 3, with these results complemented by
3 Figure 6.

4 For the Swiss dataset, the best model fit is obtained by a quantum amplitude model with an
5 ADLD value function. Notably, there is a high degree of non-linearity, with all ADLD functions
6 resulting in a significant improvement over models with a linear difference value function. If only
7 linear differences are considered, DFT results in the best model fit. Gains over the LD value
8 function are also obtained through the use of S+ and μ -RRM value functions for the quantum
9 amplitude model. Whilst the model results obtained from the quantum Hamiltonian models are
10 similar to those of the utility models, DFT and quantum amplitude models both offer substantial
11 improvements in model fit, for all value functions other than a quantum amplitude model with
12 linear differences.

13 Similar results are also obtained for the UK value of time data, with DFT again substantially
14 outperforming all other models when linear differences are used. This suggests that a standard
15 DFT model can account for non-linearity, as the difference disappears upon moving to ADLD
16 value functions, for which very similar log-likelihoods are obtained across all four models. The
17 quantum amplitude model again gives us the best model fit across the dataset, through the use
18 of attribute-specific λ parameters in the ADLDpA value function.²² This addition results in the
19 amplitude model substantially outperforming the other models. The μ -RRM model obtains an
20 estimate for μ that is insignificantly different from 1 for the quantum amplitude model, resulting
21 in an equivalent model fit to that of the S+ value function. We again observe no difference in model
22 fit between RRM, μ -RRM and MNL as there are only two choice alternatives in all choice tasks.

23 For the UK best-worst dataset, our quantum models do not perform as well. This is particularly
24 the case for continued deliberation (when a single value is used to generate probabilities for best
25 and worst choice), for which the best performing model is the ADLD utility model. Whilst DFT
26 achieves similar model fit, neither Hamiltonian nor amplitude models perform as well as the utility
27 models. Notably, very similar log-likelihoods are obtained for MNL, RRM and μ -RRM. We again
28 observe that DFT models perform best for linear difference value functions, with a substantial
29 difference observed for the UK best-worst independent deliberation models. This advantage is
30 reduced through the use of ADLD value functions, though DFT models still give the best model
31 fit.

32 Crucially, across all three datasets, the best performing quantum amplitude model achieves a
33 better model fit than the best utility model. In comparison to the quantum models, DFT performs
34 similarly for the Swiss dataset, worse for the UK value of time dataset and better for the UK best-
35 worst dataset. The only substantial difference in model fit in favour of the Hamiltonian model
36 over the amplitude model occurs when linear differences are used for the independent deliberation
37 models. This difference is reversed, however, through the use of ADLD value functions. In Table 4,
38 we also give some parameter estimates for the ADLD models run on the Swiss data (model outputs
39 for more complex specifications of these models are given in Tables 7 and 10 for the UK value of
40 time and UK best worst datasets, respectively). Whilst the outputs from quantum and DFT models

²¹Note that we do not report BIC values here, as for the Swiss dataset, the best-fitting version of each model has the same number of parameters, and for the UK datasets, we provide more complex versions of the models in later subsections.

²²Note that ADLDpA value functions were tested on both the Swiss and UK best-worst datasets but did not result in a significant improvement in model fit for any of the model types.

TABLE 3 : Log-likelihoods for basic versions of logit, DFT, quantum Hamiltonian and quantum amplitude models across all three datasets

Dataset	Value function	Model Type											
		Utility		Decision Field Theory		Quantum Hamiltonian		Quantum Amplitude					
		pars.	LL	pars.	LL	pars.	LL	pars.	LL				
Swiss	LD	5	-1,667.97	6	-1,575.40	6	-1,666.92	6	-1,682.83				
	ADLD	7	-1,631.46	7	-1,570.56	7	-1,638.96	7	-1,569.05				
	S+	5	-1,667.97					6	-1,587.00				
	μ -RRM	6	-1,667.97					7	-1,576.56				
UK value of time	LD	3	-9,603.17	4	-9,390.42	4	-9,412.23	4	-9,524.21				
	ADLD	5	-9,306.86	5	-9,309.98	5	-9,310.32	5	-9,313.73				
	ADLDpA	7	-8,936.61	6	-8,982.05	6	-9,026.91	7	-8,790.80				
	S+	3	-9,603.17					4	-9,369.61				
μ -RRM	4	-9,603.17					5	-9,369.61					
UK best-worst [continued deliberation]	LD	10	-5,802.67	13	-5,788.36	13	-5,831.05	11	-5,850.54				
	ADLD	12	-5,777.57	14	-5,780.56	14	-5,818.60	12	-5,802.22				
	S+	10	-5,803.97					11	-5,812.90				
	μ -RRM	11	-5,802.25					12	-5,812.90				
UK best-worst [independent deliberation]	LD	10	-5,780.34	13	-5,656.16	14	-5,818.74	11	-5,868.75				
	ADLD	12	-5,668.36	14	-5,648.68	15	-5,818.74	12	-5,660.84				
	S+	10	-5,815.69					11	-5,683.49				
	μ -RRM	11	-5,724.44					12	-5,683.49				

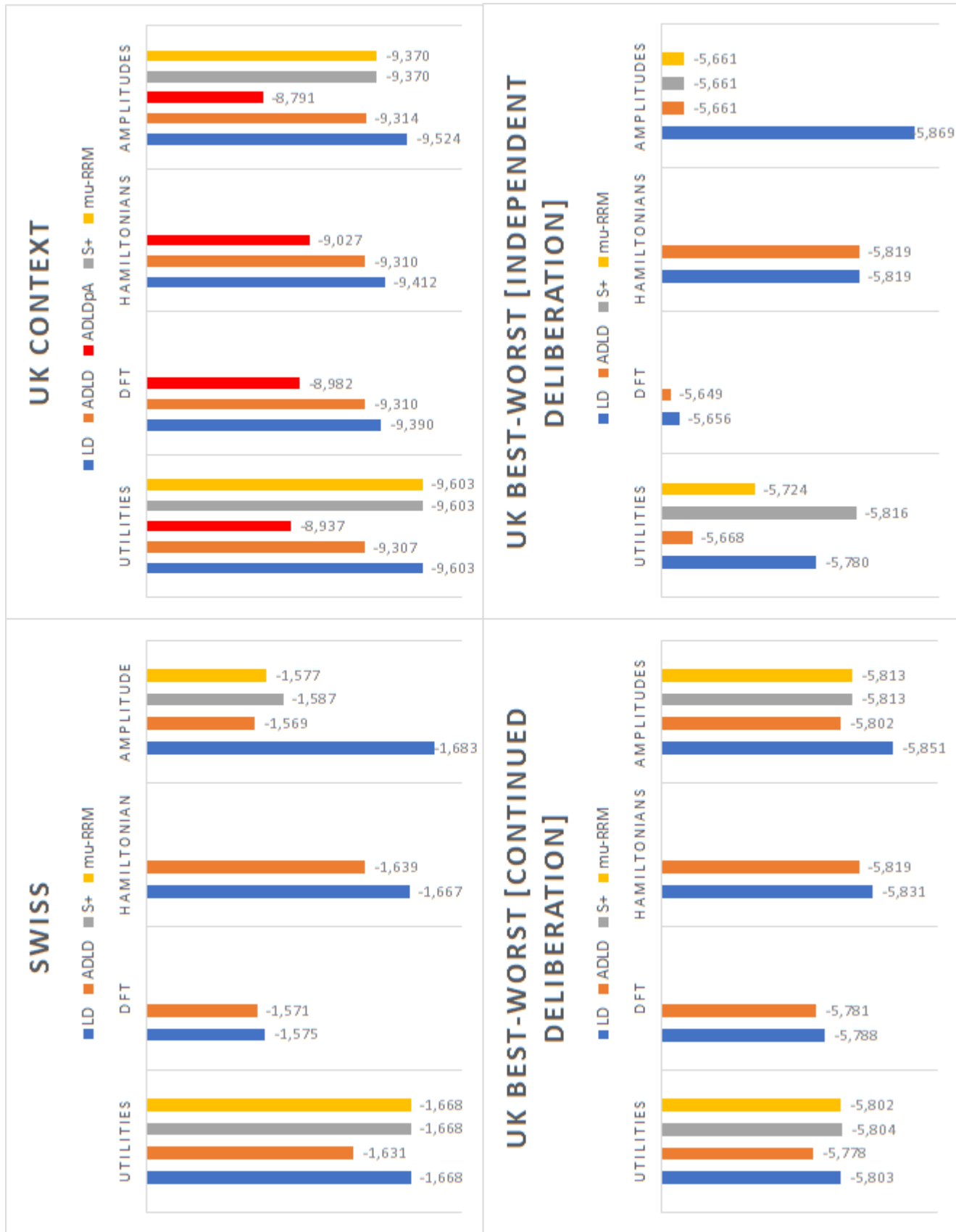


FIGURE 6 : The log-likelihoods of the basic models across the three datasets

1 cannot be translated into measures such as the value of travel time, we can obtain an indication for
 2 the relative importance (RI) of the different attributes by dividing the parameter estimates by the
 3 sum of the absolute value of all attribute coefficients. Thus, the relative importance for attribute l
 4 is defined:

$$RI_l = \frac{|\beta_l|}{\sum_{k=1}^K |\beta_k|}, \quad (20)$$

5 where $k = 1, \dots, K$ is an index across attributes. All models find significant estimates with the
 6 expected sign for all four attributes, and no significant bias between alternatives 1 and 2. The
 7 quantum amplitude model gives similar relative importance weights to the utility model, whereas
 8 the DFT and Hamiltonian models give less importance to cost, instead giving a higher weight to
 9 the number of changes (β_{CH}). The quantum amplitude model has a better fit than the Hamiltonian
 10 model, however, suggesting that differences in attribute importance across the models may not be
 11 the driving force behind the differences in model fit.

12 Additionally, all models find significant estimates for λ_1 , which is unsurprising given that all
 13 models with ADLD value functions offer a significant improvement in model fit over the corre-
 14 sponding LD value function models. The non-linearity captured by the models utilising ADLD
 15 functions is demonstrated for differences in travel time between alternatives in Figure 7. In this
 16 figure, the y-axis shows the ‘relative contribution’ to Δ_{ij} , which is defined as Equation 14 but with-
 17 out the multiplication by β_k (thus it is equivalent to $w_{x_{ijk}} \cdot (x_{ik} - x_{jk})$), which allows us to compare
 18 the impact of the non-linearity across the models. These results suggest that the quantum models
 19 find a stronger damping effect, resulting in greater differences having less of an impact in these
 20 models relative to their impact in the DFT and logit models, which have nearly identical satiation
 21 rates.

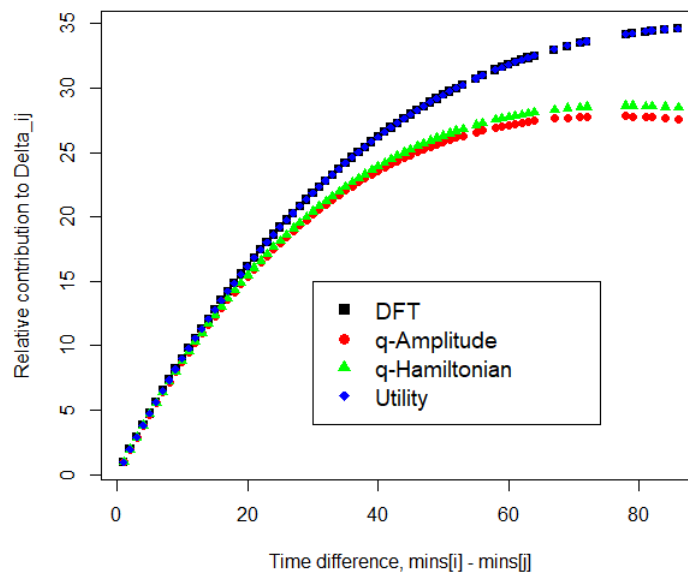


FIGURE 7 : The non-linearity for time differences in the Swiss models

TABLE 4 : Parameter estimates from the models for the Swiss dataset with ADLD value functions, with rel. weight giving the relative importance of the different attributes

		Utility	DFT	q-Hamiltonian	q-Amplitude
Parameters		7	7	7	7
Log-likelihood		-1,631.46	-1,570.56	-1,638.96	-1,569.05
β_{TT}	est.	-0.1231	-3.8682	-0.0300	-0.4071
	rob. t-rat.	-5.00	-9.35	-9.55	-3.82
	rel. weight	8.3%	5.8%	6.3%	6.8%
β_{COST}	est.	-0.3575	-12.7524	-0.0883	-1.3585
	rob. t-rat.	-4.17	-6.55	-5.82	-3.23
	rel. weight	24.1%	19.1%	18.5%	22.6%
β_{HW}	est.	-0.0257	-1.2633	-0.0100	-0.1051
	rob. t-rat.	-7.68	-5.77	-14.54	-4.23
	rel. weight	1.7%	1.9%	2.1%	1.7%
β_{CH}	est.	-0.9773	-48.9351	-0.3496	-4.1473
	rob. t-rat.	-5.94	-6.49	-15.04	-4.42
	rel. weight	65.9%	73.2%	73.2%	68.9%
λ_1	est.	0.7560	0.0027	0.4300	0.0325
	rob. t-rat.	2.29	3.07	7.81	4.35
λ_2	est.	0.0859			1.0000
	rob. t-rat.	0.79			fixed
δ_1	est.	-0.0150	-1.1200		0.6400
	rob. t-rat.	-0.37	-0.37		2.06
δ_2	est.	0.0000	0.0000		0.6500
	rob. t-rat.	fixed	fixed		2.12
δ_{12}	est.			-0.0025	
	rob. t-rat.			-0.22	
σ_ϵ	est.		1.0000		
	rob. t-rat.		fixed		
t	est.		5.9293		
	rob. t-rat. (vs. 1)		5.96		
h_{11}	est.			0.9051	
	rob. t-rat. (vs. 1)			2.37	

1 5.2. Extension to complex value-functions

2 Proper to a quantum-like approaches, the value functions (see Section 3.4), which build up the
3 amplitudes, Equation (3) and drive the Hamiltonians, Equation (7), need not to be restricted to real-
4 valued expressions. This increased flexibility allows for interactions between different components
5 within an evaluation of an alternative.

6 5.2.1. Specification

7 Whilst there are many different possibilities for how to construct real and imaginary parts within a
8 value function, in this section we consider only simple specifications where the alternative specific
9 constants (δ) and attribute comparisons (Δ) are either real or imaginary. For imaginary parts,
10 we simply multiply the corresponding component by i . Thus, for example, in the Hamiltonian
11 model, Equation 7 becomes $h_{ij} = \delta_{ij} + i \cdot \Delta_{ij}$, for a model with real alternative specific constants
12 and imaginary valued attribute differences. This gives us four alternative specifications for the
13 Hamiltonian models. For the amplitude model, the equivalent model with real alternative specific
14 constants and imaginary valued attribute differences is (for the UK value of time dataset):

$$\psi_1 = (\delta_1 + i \cdot wtc_{12} \cdot tc_{12} + i \cdot wtt_{12} \cdot tt_{12}) / \sqrt{\mathcal{N}} \quad (21)$$

$$\psi_2 = (\delta_2 + i \cdot wtc_{21} \cdot (-tc_{12}) + i \cdot wtt_{21} \cdot (-tt_{12})) / \sqrt{\mathcal{N}} \quad (22)$$

15 with tc_{12} the difference in travel cost between alternatives 1 and 2, tt_{12} the difference in travel
16 times between alternatives 1 and 2, multiplied by their similarity weightings (which are defined in
17 Equation 15). Finally, we have:

$$\mathcal{N} = |\delta_1 + i \cdot wtc_{12} \cdot tc_{12} + i \cdot wtt_{12} \cdot tt_{12}|^2 + |\delta_2 + i \cdot wtc_{21} \cdot (-tc_{12}) + i \cdot wtt_{21} \cdot (-tt_{12})|^2, \quad (23)$$

18 which ensures that the sum over the probabilities of each alternative equals 1. We only have two
19 different real-imaginary combinations for the amplitude models, as a result of the use of the norm
20 in Equations (4) and (23), implying $|i \cdot \delta_i + \sum_{i \neq j}^J \Delta_{ij}|^2 = |\delta_i + i \cdot \sum_{i \neq j}^J \Delta_{ij}|^2$ and also
21 $|i \cdot \delta_i + i \cdot \sum_{i \neq j}^J \Delta_{ij}|^2 = |\delta_i + \sum_{i \neq j}^J \Delta_{ij}|^2$. For the Hamiltonian models, each of the four real-imaginary
22 combinations leads to a different dynamical evolution as a result of Equation (8).

23 5.2.2. Results

24 The results of each of these specifications is given in Table 5 for the ADLD value function model
25 for each dataset.

26 For the Hamiltonian models, the addition of imaginary differences (Im- Δ) has a negative impact
27 for the Swiss and UK value of time datasets, resulting in a far inferior model fit. The alternative
28 specific constants (which are not significant for the Swiss dataset, see Table 4) have little effect on
29 the model, with the consequence that there is little impact on model fit by changing from real to
30 imaginary alternative specific constants. For the UK best-worst dataset, we observe far superior
31 model fits through the use of imaginary attribute differences, with the improvement for the inde-
32 pendent deliberation model resulting in the Hamiltonian model becoming more similar in model
33 fit in comparison to the quantum amplitude, utility and DFT model results for the same data. For
34 the amplitude models, we observe a better model fit in all cases for real-real/imaginary-imaginary
35 combinations. Overall, these results suggest that there is ample scope for future exploration of
36 alternative specifications of real and imaginary parts within quantum choice models.

TABLE 5 : Results from models incorporating real and imaginary parts for both q-Hamiltonian and q-Amplitude models

	Re- δ Re- Δ	Re- δ Im- Δ	Im- δ Re- Δ	Im- δ Im- Δ
	q-Hamiltonian	q-Hamiltonian	q-Hamiltonian	q-Hamiltonian
Swiss	7 -1,638.96	7 -1,785.75	7 -1,638.88	7 -1,785.89
UK value of time	6 -9,026.91	6 -9,395.86	6 -9,028.27	6 -9,394.86
UK best-worst [continued]	14 -5,818.60	14 -5,792.70	14 -5,814.29	14 -5,811.96
UK best-worst [independent]	15 -5,818.74	15 -5,684.40	15 -5,762.21	15 -5,810.28
	q-Amplitude	q-Amplitude	q-Amplitude	q-Amplitude
Swiss	7 -1,569.05	7 -1,569.56	7 -1,569.56	7 -1,569.05
UK value of time	7 -8,790.80	7 -8,967.92	7 -8,967.92	7 -8,790.80
UK best-worst [continued]	12 -5,802.22	12 -5,834.97	12 -5,834.97	12 -5,802.22
UK best-worst [independent]	12 -5,660.84	12 -5,673.93	12 -5,673.93	12 -5,660.84

1 5.3. Models with quantum rotation: contextual and ordering effects in the UK value of time 2 dataset

3 Thus far, we have only implemented quantum choice models without the use of quantum rotations.
4 In Section 3.3, we demonstrate how ‘a change of perspective’ in a decision task can be represented
5 within a quantum choice model by performing a quantum rotation on the belief state. In this
6 section, we give the results of models incorporating rotations for contextual and ordering effects in
7 the UK value of time dataset.

8 This theoretically works well for the UK value of time dataset, which has some choice sets
9 with the cheaper alternative shown first, and some with the faster alternative shown first, as well
10 as having cost sometimes on top and sometimes at the bottom. Whilst we could again use a full
11 set of different parameters for the four different scenarios, these ordering effects have previously
12 been found to be significant (Hess et al., 2017), making this an appropriate dataset to test quantum
13 rotations.

14 5.3.1. Model specification

15 Contextual effects such as described above can be captured in both our amplitude and Hamiltonian
16 quantum models through a supplementary rotation for a switched option order and/or switched
17 textual representation. The sizes of the two rotation angles give an immediate process-based as-
18 sessment of the location order bias and the textual phrasing bias.

19 In the Hamiltonian model, there is a Hamiltonian operator for the basic change in belief state
20 due to the different values of the attributes of the two alternatives, and additionally an effect from
21 a supplementary rotation for switched option order and for switched textual representation. The
22 order effect is implemented by a rotation of the belief state $\Psi = (\psi_1, \psi_2)$ in the Hilbert space where
23 the first component ψ_1 represents the belief amplitude for alternative 1 and the second amplitude
24 ψ_2 sustains the choice for alternative 2. Thus, for the reference configuration, ‘option order’ (Op-
25 tOrd=1) and ‘time-cost order’ (TCOrd=1), we have a basic Hamiltonian (H_{11}) set up as before,
26 based on Equation 6. This is again a basic parametrised Hadamard gate, that is commonly used to
27 implement the dynamics in a binary choice (Busemeyer et al., 2011). When the time-cost order re-

1 mains as in the reference configuration (TCOrd=1) while the option order is switched (OptOrd=2),
 2 the basic Hamiltonian is complemented with a small rotation over an angle ϑ_{LR} to implement the
 3 bias for option ordering. When on the other hand, only the time-cost order is changed with respect
 4 to the reference configuration and the option order remains unchanged (TCOrd=2, OptOrd=1),
 5 the basic Hamiltonian is again complemented with a rotation but with different angle size ϑ_{Phr} .
 6 When both time-cost order and the option order are changed with respect to the reference configu-
 7 ration, (OptOrd=2, TCOrd=2), the basic Hamiltonian is now complemented with the effect of both
 8 rotations with the combined angle $\vartheta_{LR} + \vartheta_{Phr}$. Thus, the respective Hamiltonians are given by:

$$H_{11} = \begin{pmatrix} h_{11} & \delta_{12} + \Delta_{12} \\ \delta_{12}^* + \Delta_{12}^* & -1 \end{pmatrix} \quad (24)$$

$$H_{12} = H_{11} + \vartheta_{LR} \sigma_y \quad (25)$$

$$H_{21} = H_{11} + \vartheta_{Phr} \sigma_y \quad (26)$$

$$H_{22} = H_{11} + (\vartheta_{LR} + \vartheta_{Phr}) \sigma_y. \quad (27)$$

9 Note that this is equivalent to adjusting the off-diagonals of H_{11} , with, for example, the upper and
 10 lower off-diagonals of H_{12} being $\delta_{12} + \Delta_{12} - i \vartheta_{LR}$ and $\delta_{12}^* + \Delta_{12}^* - i \vartheta_{LR}$, respectively. Conse-
 11 quently, for this implementation of the Hamiltonian model, the process of attribute comparison
 12 and ordering bias occurs simultaneously (addition on Hamiltonian level). The choice process
 13 could also be modelled sequentially by separating the Hamiltonian evolution operator, Equation
 14 (8), from the rotation operator, Equation (12), and applying them consecutively to the initial belief
 15 state. This method can also be used for the amplitude-approach, under which the attribute values of
 16 the two alternatives initially determine the basic reference probability amplitude, while dedicated
 17 rotations implement the bias process for switched option order and for switched textual represen-
 18 tation. Thus, in principle, we implement the same respective rotation operators (based on Equation
 19 12), for time-cost ordering and option ordering;

$$R_{Phr} = e^{-i\vartheta_{Phr} \sigma_y}, \quad (28)$$

$$R_{LR} = e^{-i\vartheta_{LR} \sigma_y} \quad (29)$$

20 in both the amplitude model and Hamiltonian model.

21 We compare different levels of complexity for each of the different model structures. We
 22 test three variations for contextual ‘changes in perspective’ for both the Hamiltonian and ampli-
 23 tude models as well as trying ‘separate’ parameter models where a set of attributes (based on the
 24 ADLDPa basic models) are estimated for each of the four contextual framings. Thus, we have the
 25 following five specifications:

- 26 1. A basic model. These models correspond to those given by the ADLDPa models in Table 3.
- 27 2. A model where a shift is made to Δ_{12} , such that the constant δ_{LR} is added if (OptOrd=2) and
 28 the constant δ_{Phr} is added if (TCOrd=2). For the Hamiltonian model, this corresponds to
 29 Equations (24-27) with the use of σ_x in place of σ_y .
- 30 3. A model where an *imaginary* valued shift is made to Δ_{12} , such that $i \cdot \delta_{LR}$ is added if (Op-
 31 tOrd=2) and $i \cdot \delta_{Phr}$ is added if (TCOrd=2). For the Hamiltonian model, this corresponds to
 32 Equations (24-27). The use of imaginary numbers here means that this version cannot be
 33 implemented in the utility and DFT models.

- 1 4. A model with the application of a quantum rotation of R_{Phr} as defined by Equation 28 if
 2 (TCOrd=2), and a rotation of R_{LR} (see Equation 29) if (OptOrd=2). This results in the
 3 estimation of two additional parameters, ϑ_{Phr} and ϑ_{LR} .
- 4 5. A ‘separate’ model, in which the basic models are applied separately to subsets of the data
 5 corresponding to each contextual scenario. As we have four different scenarios, this results
 6 in a fourfold increase in the number of parameters for each model.

7 5.3.2. Results

8 The results of all possible specifications are given for each of the four model frameworks in Table
 9 6.

TABLE 6 : Log-likelihood and BIC performance of Logit, DFT, Hamiltonian and Amplitude models for the UK-context paradigm, with models 2-5 also giving the improvement in log-likelihood over model 1.

		Logit	DFT	q-Hamiltonian	q-Amplitude
[1] Basic model	pars.	7	6	6	7
	LL	-8,936.61	-8,982.05	-9,026.91	-8,790.80
	BIC	17,941	18,022	18,112	17,649
[2] Context shifts added to Δ_{12}	pars.	9	8	8	9
	LL	-8,927.59	-8,976.53	-9,018.09	-8,783.64
	LL improvement	9.01	5.52	8.82	7.16
	BIC	17,942	18,030	18,113	17,654
[3] (Im) Context shifts added to Δ_{12}	pars.			8	9
	LL			-9,016.93	-8,789.96
	LL improvement			9.97	0.84
	BIC			18,111	17,666
[4] Rotation operators, R_{Phr} and R_{LR}	pars.			8	9
	LL			-9,017.76	-8,779.71
	LL improvement			9.14	11.09
	BIC			18,112	17,646
[5] Separate pars.	pars.	28	24	24	28
	LL	-8,909.48	-8,959.43	-8,990.00	-8,769.81
	LL improvement	27.12	22.62	36.91	20.99
	BIC	18,088	18,150	18,211	17,809

10 For all specifications, the amplitude model outperforms the utility model, which in turn has a
 11 better model fit than DFT and the Hamiltonian models. For all model frameworks, it appears that
 12 using separate sets of parameters instead of a basic model results in an improvement in model
 13 fit but a worse BIC. Whilst the quantum rotation models are not as successful as capturing the
 14 difference between the contextual situations as models with separate parameters, these models
 15 return favourable BICs as they only have two additional parameters. Notably, the best performing
 16 Hamiltonian model (in terms of BIC) implements an imaginary shift, as defined by Equations
 17 (24-27), and the model with the overall best BIC value is obtained with an amplitude model with
 18 rotation operators. The key parameter outputs for these models are given in Table 7.

TABLE 7 : Key model outputs from the context models with shifts or rotations for a change in context

Model	Version	Gain in Log-likelihood	Rel. importance of time (£/hour)	$\delta_{LR}/\vartheta_{LR}$		$\delta_{Phr}/\vartheta_{Phr}$	
				Estimate	Rob. t-rat.	Estimate	Rob. t-rat.
Utility	2	9.01	6.49	-0.1467	-3.81	0.0464	1.45
DFT	2	5.52	3.58	-0.3133	-2.99	0.0957	1.13
q-Hamiltonian	2	8.82	3.63	-0.0479	-3.88	0.0042	0.41
	3	9.97	3.65	-0.0995	-3.61	0.1022	3.02
	4	9.14	3.63	-0.0419	-3.85	0.0083	0.92
q-Amplitude	2	7.16	5.26	-10.3154	-3.52	2.3966	0.97
	3	0.84	5.26	-38.6215	-0.69	59.7161	0.71
	4	11.09	5.25	-0.0342	-4.29	0.0147	2.09

1 Crucially, all but one model show a negative estimate for $\delta_{LR}/\vartheta_{LR}$, which means that the probability
2 of alternative 2 increases when we move from option order 1 to option order 2. This result is in line
3 with the original test and confirms the presence of a shift in left-right bias as a result of changing
4 whether the cheaper and slow alternative appears on the left or the right. For most of the models,
5 we also confirm that there is no effect of changing the order of appearance for the attributes. Table
6 6 also gives the ‘relative importance of travel time with respect to travel cost’, which is defined as
7 the ratio of the time parameter estimate divided by the cost parameter estimate, multiplied by 60
8 (see further detail in Hancock et al. (2018) on how this measure can be interpreted). Whilst this
9 does not correspond to welfare measures (as all models use asymmetric decay functions), these
10 values give us an indication as to whether a decision-maker will more likely choose a fast or cheap
11 alternative. In comparison to the utility model, both DFT and quantum models assign a lower
12 importance to travel time.

13 By considering the parameter outputs for version 4 (quantum rotation) models, we can also
14 calculate the estimated rotation matrices R_{Phr} and R_{LR} . For the Hamiltonian (Ham) and amplitude
15 (Amp) models, the rotation matrices for changing from having the cheaper alternative on the left
16 (first) to on the right (second) are:

$$R_{LR_{Ham}} = \begin{bmatrix} 0.999 & -0.042 \\ 0.042 & 0.999 \end{bmatrix}, R_{LR_{Amp}} = \begin{bmatrix} 0.999 & -0.034 \\ 0.034 & 0.999 \end{bmatrix}, \quad (30)$$

17 and the estimates for the quantum rotation matrices for changing from having the travel time first
18 to having the travel cost first are:

$$R_{Phr_{Ham}} = \begin{bmatrix} 0.999 & 0.008 \\ -0.008 & 0.999 \end{bmatrix}, R_{Phr_{Amp}} = \begin{bmatrix} 0.999 & 0.015 \\ -0.015 & 0.999 \end{bmatrix}. \quad (31)$$

19 This results in a shift towards alternative two through the use of R_{LR} and a small shift towards
20 alternative one through the use of R_{Phr} .

21 5.4. Contextual and ordering effects in the UK best-worst data

22 The best-worst dataset also presents a suitable paradigm for the implementation of a quantum
23 rotation, as it is possible that the influence of individual attributes may differ between the case
24 of choosing the best alternative and the case of choosing the worst alternative (Giergiczny et al.,
25 2017).

1 5.4.1. Model specification

2 In the quantum-like approach, this changed perspective can be obtained by modifying the an-
 3 gle over which the basis vectors representing the choice of the worst alternative, $|\text{Alt}_i \text{ worst}\rangle$,
 4 $|\text{Alt}_j \text{ worst}\rangle$, are rotated with respect to $|\text{Alt}_i \text{ best}\rangle$, $|\text{Alt}_j \text{ best}\rangle$. This rotation changes the norm of
 5 the projected amplitudes (see Figure 3) and thus modifies the probability for choosing the worst
 6 alternative, see Equation (1). Formally, the belief state for choosing the worst alternative, Ψ_{worst} , is
 7 obtained by applying the rotation matrix R , Equation (12), to the residual belief state after having
 8 chosen the best alternative:

$$\Psi_{\text{worst}} = R\Psi_{\text{Resid. best}}, \quad (\text{Best} - \text{Worst rotation}) \quad (32)$$

9 where $\Psi_{\text{Resid. best}}$ is a renormalised vector of the belief state Ψ_{best} over the remaining choice alter-
 10 natives. One can easily verify that a rotation over an angle $\pi/2$ according to the axis of rotation
 11 $n_y = 1$ results in the ‘basic inversion’ condition, Equation (19). Mathematically, this rotation si-
 12 multaneously causes a change in both underlying preferences towards alternatives and a change in
 13 how deterministic the choice is. In our empirical application, we test the basic inversion, Equation
 14 (19), and the more general quantum rotation, Equation (32). Naturally, if there is a mere classical
 15 inversion of amplitudes, the parameters will tend towards those that generate Equation (19).

16 Under both the Hamiltonian and amplitude models, we assume a three dimensional complex
 17 Hilbert space for the belief states, $\Psi = (\psi_1, \psi_2, \psi_3)$, in which the respective components constitute
 18 the support for the respective alternatives. In the Hamiltonian approach, the decision process for
 19 the choice of the best alternative starts from an initial state Ψ_0 :

$$\Psi_0 = \begin{pmatrix} \alpha \\ \beta \\ \gamma \end{pmatrix}, \quad (33)$$

20 which can be configured as unbiased $|\alpha| = |\beta| = |\gamma| = 1/\sqrt{3}$. A relative phase can be implemented
 21 on the amplitudes to differentiate their engagement with the unitary evolution operator, Equation
 22 (8), or a non-process bias with respect to specific alternatives by setting $|\alpha| \neq |\beta| \neq |\gamma|$. The initial
 23 belief state is subject to change according to the Hamiltonian for choice of the best alternative:

$$H = \begin{pmatrix} h_{11} & h_{12} & h_{13} \\ h_{12}^* & 0 & h_{23} \\ h_{13}^* & h_{23}^* & h_{33} \end{pmatrix}. \quad (34)$$

24 The expression of the Hamiltonian can be considered as the superposition of three parametrised
 25 Hadamard gates which respectively implement the pairwise comparison process of attributes of the
 26 alternatives, Equation (7).

27 In the amplitude model, the summed attribute differences are implemented directly into the
 28 probability amplitudes for each alternative:

$$\psi_1 = \left(\delta_1 + e^{i\phi_{bw}} (\Delta_{12} + \Delta_{13}) \right) / \sqrt{\mathcal{N}}, \quad (35)$$

$$\psi_2 = \left(\delta_2 + e^{i\phi_{bw}} (\Delta_{21} + \Delta_{23}) \right) / \sqrt{\mathcal{N}}, \quad (36)$$

$$\psi_3 = \left(\delta_3 + e^{i\phi_{bw}} (\Delta_{31} + \Delta_{32}) \right) / \sqrt{\mathcal{N}}, \quad (37)$$

1 where \mathcal{N} renders the belief state normalized to 1, similarly to Equation (23). The relative phase
 2 ϕ_{bw} between the bias component δ_j and the attribute differences ($\Delta_{ji} + \Delta_{jk}$) implements a differ-
 3 ence in processing for both factors.

4 In both of the quantum models that we implement, we also explore the inclusion of a ‘propor-
 5 tion’ parameter for the possibility that a respondent would reverse the processing order of choos-
 6 ing the best and worst alternatives. The UK-best/worst survey allows the respondent to either first
 7 choose the best alternative and then follow this by selecting the worst between the two remaining
 8 alternatives, or vice versa, starting with choosing the worst alternative before then choosing the
 9 best out of the remaining two alternatives. The proportion parameter expresses the proportion of
 10 choice processes that are taken in reverse order, by weighting the theoretical choice probabilities
 11 from models for both orders (‘best then worst’ and ‘worst then best’). Whilst there are many pos-
 12 sibilities for specifications for models that implement a ‘proportion’ parameter, we only test the
 13 most basic specification in our empirical application, under which there are no other additional pa-
 14 rameters. Thus if a decision-maker considers worst and then best, Ψ_{worst} is generated using $-\delta_{ij}$
 15 and $-\Delta_{ij}$ in place of δ_{ij} and Δ_{ij} in the Hamiltonian model. For the amplitude model, $\Delta_{ij} \neq \Delta_{ji}$,
 16 thus we use $-\delta_i$ and Δ_{ji} in place of δ_i and Δ_{ij} . Then, we generate a rotation matrix R that translates
 17 best to worst, and use R^{-1} for the translation from worst to best.

18 In this application, we explore basic models for both ‘independent’ and ‘continued’ delibera-
 19 tion assumptions. Given the various extensions to these models discussed above, we consider four
 20 further possibilities. This gives us a total of six different specifications for the quantum choice
 21 models (and three for the utility and DFT models, which do not implement quantum rotations).
 22 These six possibilities are:

- 23 1. A basic structure for each model based on independent deliberations, meaning that best and
 24 worst choice probabilities are calculated independently with worst choice using only the two
 25 unchosen alternatives within the value functions (thus not using the attribute values from the
 26 alternative chosen as best). In the first implementation of independent deliberations, we use
 27 the same set of estimated parameters for best and worst choice. To estimate the probability
 28 for worst choice, we simply calculate the probability of the other alternative being chosen
 29 as (second) best. The utility, DFT and amplitude models here correspond to the indepen-
 30 dent deliberation ADLD models given in Table 3. For the Hamiltonian model, we instead
 31 implement imaginary attribute differences,²³ which corresponds to the best performing (in-
 32 dependent deliberation) Hamiltonian model from Table 5.
- 33 2. The second method again uses the assumption of independent deliberations, but now allows
 34 for a completely ‘separate’ set of parameters for the best choices compared to the worst.
 35 This is equivalent to running two separate models where the dataset is split into two subsets:
 36 one with only the best alternative choice tasks and one with only the worst alternative choice
 37 tasks. Note that whilst this effectively doubles the number of estimated parameters, two
 38 DFT parameters are dropped as there is no significant impact of including feedback matrix
 39 parameters for the worst choice (as is often the case when choosing between two alternatives,
 40 see Appendix). Additionally, the Hamiltonian model estimates 2 diagonal elements for the
 41 Hamiltonian for best choice and 1 for the Hamiltonian for worst choice. Consequently, we
 42 do not need these 3 parameters twice for separate parameter models of best and worst choice.

²³Note that all Hamiltonian models in this section are implemented in this way.

- 1 3. The third specification is based on the assumption of continued deliberation. This means
 2 that the probabilities for best and worst choice are generated simultaneously through the
 3 use of a single value function. We assume basic inversions for all models meaning that the
 4 same attributes are important for best and worst choice. These models correspond to the
 5 continued deliberation ADLD models given in Table 3, with the Hamiltonian model again
 6 using imaginary attribute differences, corresponding to the result in Table 5.
- 7 4. The fourth model uses continued deliberations, but also allows for the application of a quan-
 8 tum rotation, R (see Equation 32, that is defined by Equation 12). To estimate R , we need to
 9 find the relative importance of the three Pauli matrices. In all cases, we find that the impact
 10 of including a third Pauli matrix is insignificant, and thus two additional parameters are esti-
 11 mated, ϑ and ω ,²⁴ where $R = e^{-i\vartheta(n_1\sigma_1+n_2\sigma_2)}$, $n_1 = \sin(\omega)$, $n_2 = \cos(\omega)$ and $n_3 = 0$. For
 12 the Hamiltonian models, $n_x = 0$, and for the amplitude models, $n_z = 0$. Note that just a sin-
 13 gle rotation matrix is used here, meaning that the model uses the same rotation to adjust the
 14 amplitudes for the two remaining alternatives, regardless of which pair is left. This results in
 15 the assumption that the same adjustment happens for $(\text{Alt}_1 \rightarrow \text{Alt}_2)$, $(\text{Alt}_1 \rightarrow \text{Alt}_3)$ and $(\text{Alt}_2$
 16 $\rightarrow \text{Alt}_3)$.
- 17 5. The fifth model is equivalent to the fourth model, except that it also estimates a ‘proportion’
 18 parameter. This parameter estimates the percentage of decision-makers who ‘choose best
 19 then worst’ or ‘worst then best’.
- 20 6. The final model is equivalent to the fifth model, with the exception that two different rota-
 21 tion matrices are estimated through the use of two different axes specified by the parameter
 22 ω , one for the rotation from best to worst (ω_{bw}), and the other for the rotation from worst
 23 to best (ω_{wb}). Additionally, the Hamiltonian model no longer assumes an indifferent initial
 24 belief state. Instead, we set $\psi_0 = (1/\sqrt{3}, e^{i s}/\sqrt{3}, e^{-i s}/\sqrt{3})$, where s is an estimated param-
 25 eter. This results in two additional parameters for the Hamiltonian model and one for the
 26 amplitude model. The ‘worst to best’ rotation matrices are then set as $R_{wb} = e^{i\vartheta(n_x\sigma_x+n_y\sigma_y)}$,
 27 where the weights n_x and n_y are estimated with ω_{wb} . Consequently, $R_{wb} = R_{bw}^{-1}$ if $\omega_{wb} = \omega_{bw}$.

28 5.4.2. Results

29 The results of these models are given in Table 8. Given the complex likelihood structure, we
 30 use an initial parameter search algorithm based on the heuristic for non-linear global optimisation
 31 developed by Bierlaire et al. (2010) in an attempt to reduce the risk of convergence to poor local
 32 optima. For all of the quantum models, we try the four different specifications using real and
 33 imaginary numbers, as tested in Table 5. For brevity, we show just the best-fitting model in each
 34 case, which is a model with $\text{Re-}\delta_{ij}$ and $\text{Im-}\Delta_{ij}$ for all of the models that incorporate quantum
 35 rotations.

36 Unsurprisingly, every model finds a significant improvement in model fit by having a separate
 37 set of parameters for the best alternatives compared to the worst alternatives (in line with the results
 38 of Giergiczny et al. 2017). This suggests that the relative sensitivities to the different attributes for
 39 a best alternative are not necessarily the same as the relative sensitivities to the different attributes
 40 for a worst alternative. The overall best-fitting model in terms of log-likelihood is the DFT model
 41 with separate parameters. However, the quantum rotation models are efficient in parameter use and

²⁴The use of ω here within a sine and cosine function ensures that $|\mathbf{n}| = 1$.

TABLE 8 : Results from models for the best-worst dataset

Standard choice models	Deliberation	Utility			DFT		
		pars.	LL	BIC	pars.	LL	BIC
[1] single set pars.	Independent	12	-5,668.36	11,444	14	-5,651.62	11,429
[2] separate pars.		24	-5,607.63	11,430	26	-5,569.04	11,371
[3] basic model	Continued	12	-5,777.57	11,663	14	-5,780.56	11,687
Quantum choice models	Deliberation	q-Hamiltonian			q-Amplitude		
		pars.	LL	BIC	pars.	LL	BIC
[1] single set pars.	Independent	15	-5,684.40	11,503	12	-5,660.84	11,429
[2] separate pars.		27	-5,657.22	11,556	24	-5,598.20	11,412
[3] basic model	Continued	14	-5,792.70	11,711	12	-5,802.22	11,712
[4] quantum rotation 1		16	-5,656.82	11,457	14	-5,742.78	11,611
[5] quantum rotation 2		17	-5,651.74	11,456	15	-5,612.08	11,359
[6] quantum rotation 3		19	-5,624.54	11,419	16	-5,611.09	11,366

1 consequently find good BIC values, with the result that the best BIC is obtained by an amplitude
2 model that uses a quantum rotation. By stepping away from ‘best = opposite of worst’, the rotation
3 models bring the performance of the continued deliberation models in line with those of the sepa-
4 rate parameter independent deliberation models. Consequently, we find that best-worst choices in
5 this dataset are ‘incompatible’: a quantum rotation is required to move from a set of basis vectors
6 for best choices to a different set of basis vectors for worst choices. Overall, the results from both
7 classical and quantum models suggest that best is not the opposite of worst, which is in line with
8 the biases present in the overall choice shares (in Table 2).

9 **Test of the quantum rotations.** Of key importance for the quantum models is to test the
10 impact of the quantum rotation matrices themselves, as the inclusion of these matrices substantially
11 improves both the Hamiltonian and amplitude models. We consider the impact of these matrices
12 by looking at the resulting probabilities generated from the application of the matrix to an initial
13 belief state. As a contrast to the rotation matrices generated by models for the UK value of time
14 dataset, it is not intuitively clear what the impact of these rotation matrices are on complex-valued
15 residual belief states, with the respective rotation matrices for the Hamiltonian (rotation 3 model)
16 and Amplitude models (rotation 2 model) being:

$$R_{Ham_{BW}} = \begin{bmatrix} 0.20 + 0.13i & 0.97 + 0.00i \\ -0.97 + 0.00i & 0.20 - 0.13i \end{bmatrix}, R_{Ham_{WB}} = \begin{bmatrix} -0.20 - 0.27i & -0.94 + 0.00i \\ 0.94 + 0.00i & 0.20 + 0.27i \end{bmatrix}. \quad (38)$$

17 and

$$R_{Amp} = \begin{bmatrix} -0.62 + 0.00i & 0.24 + 0.75i \\ -0.24 + 0.75i & -0.62 + 0.00i \end{bmatrix}. \quad (39)$$

18 We thus test these matrices by calculating their impact on the choice probabilities of each respon-
19 dent of choosing an alternative as worst, given a belief state, $\psi_{Resid.best}$, which corresponds to the

1 renormalised probability amplitudes for the remaining two alternatives following the choice of the
 2 best alternative. Vice versa, we check the choice probabilities for best alternative resulting from
 3 the application of the inverse rotation on $\Psi_{Resid.worst}$, the renormalised state for the remaining two
 4 alternatives following the choice of the worst alternative.

5 This results in Figure 8, in which the amplitudes of the two remaining alternatives - after
 6 having chosen best (left panel) and worst (right panel) alternative - are rotated to generate the
 7 choice probabilities of the alternative being chosen as worst (left panel) or best (right panel) for
 8 each individual respondent. In this figure, the black dots show how the probability changes under
 9 a basic inversion (as described by Equation 19). Under a basic inversion, best is the opposite of
 10 worst, and as a direct consequence, a belief state of, for example $\Psi_{Resid.best} = (1, 0)$ generates
 11 probabilities for worst choice equal to 0 for the upper positioned alternative, and equal to 1 for the
 12 lower positioned alternative (hence swapping the amplitude entries).

13 In both quantum models, we observe convex and concave transformations of second best (or
 14 second worst) choice probabilities into worst (or best) choice probabilities due to the rotation
 15 transformation. The impact of this rotation transformation is more easily assessed by checking the
 16 image for the value of the initial probability at 0.5, which corresponds to expressing indifference
 17 between the two remaining alternatives. In the case of a concave relation, the initial indifference
 18 results in the chosen second best (worst) alternative becoming the chosen worst (best) alternative
 19 with a higher probability. In contrast, in a convex relation, the probability of chosen second best
 20 (worst) alternative will render a lower probability for the chosen worst (best) alternative in com-
 21 parison to the basic inversion.²⁵ We can now assess the impact of the quantum rotation in the
 22 observed bias effects when choosing the status quo, i.e. Alt₁, as the worst alternative (see Table 2).
 23 Choosing the status quo as worst alternative occurs when either Alt₂ or Alt₃ are chosen as best al-
 24 ternatives, hence we must compare p(Alt₃)(vs 1) for worst (blue) with p(Alt₁)(vs 3) for worst (red)
 25 and, separately compare p(Alt₂)(vs 1) for worst (purple) with p(Alt₁)(vs 2) for worst (orange).
 26 When Alt₂ is chosen as the best alternative, the amplitude model shows a substantial bias effect
 27 against the status quo as worst choice in the ‘best then worst’ order (blue concave, red convex).
 28 When Alt₃ is chosen as the best alternative, the rotation produces the bias effect in both processing
 29 orders (purple concave and orange convex). This suggests that it is the introduction of the quantum
 30 rotation that drives the accurate recovery of the underlying observed choice shares given in Table
 31 2.

32 Under the Hamiltonian model, the bias effect is not reproduced in exactly the same manner, in
 33 particular in the ‘best then worst’ processing order. When Alt₂ is chosen as the best alternative,
 34 the Hamiltonian model renders an increased probability against the status quo as worst by shifting
 35 density for p(Alt₃)(vs 1) for worst (blue) towards lower residual probability for Alt₃ being second
 36 best, whilst shifting density for p(Alt₁)(vs 3) for worst (red) towards higher residual probability for
 37 Alt₁ being second best. In the ‘worst then best’ processing order, both models appear to use the
 38 same relative rotation transformation to produce the bias effect.

39 We also note that both models show choice order effects, although not necessarily for the same

²⁵We notice a different cause of the choice probability p(Alt₁)(vs 3) for worst alternative (red dots) in the Hamil-
 tonian and amplitude model. In the amplitude model, the lowered probability (w.r.t. basic inversion) results from
 convexity while in the Hamiltonian model it results from density (concentration towards higher probabilities in the
 residual vector). These density shifts are related to the bias parameter in the initial state in the Hamiltonian model.
 The same effect is present in the transformation for the choice probability p(Alt₃)(vs 1) for worst alternative (blue
 dots).

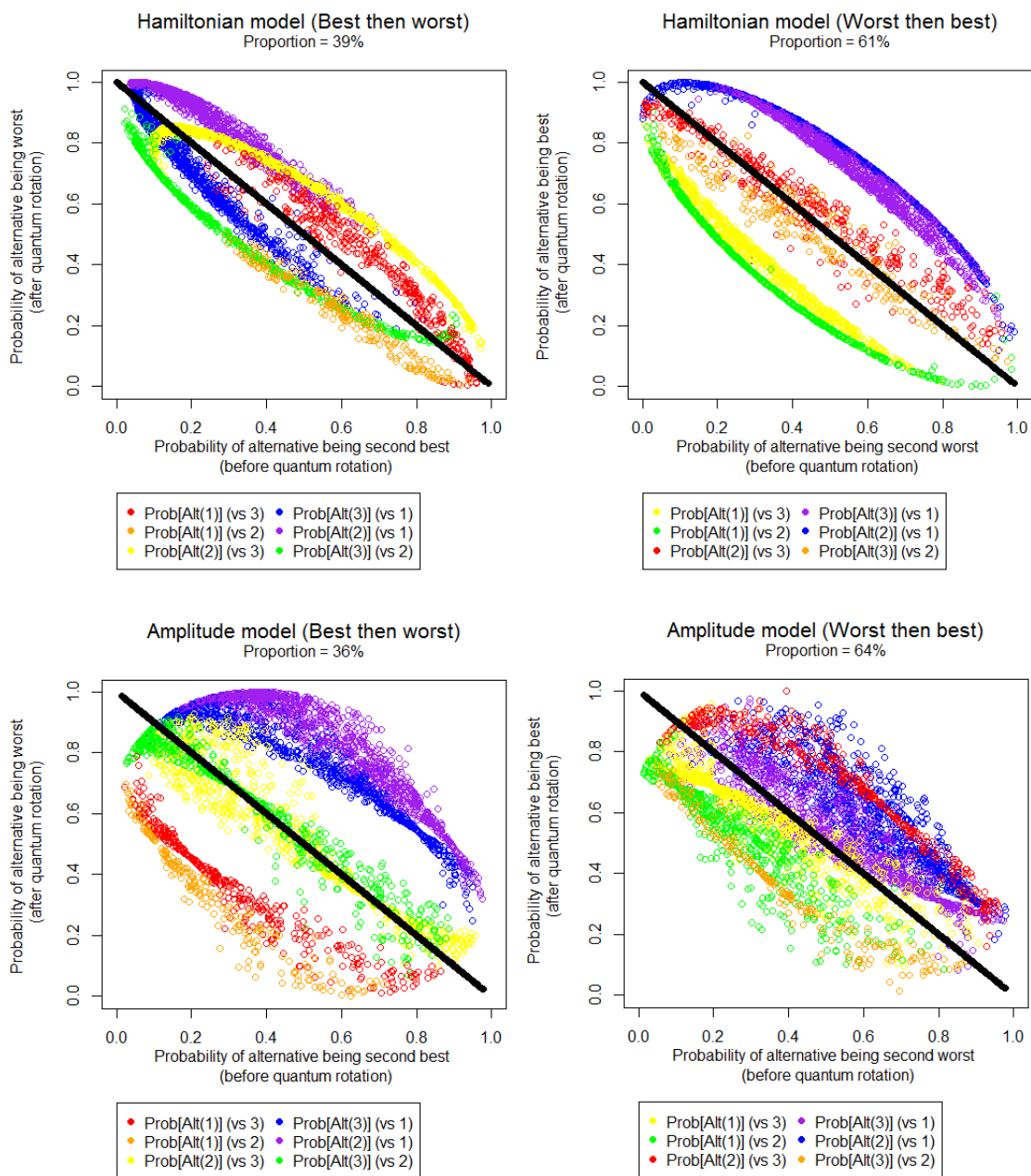


FIGURE 8 : Choice probabilities of individual decision-makers generated by the quantum rotation in the Hamiltonian model rotation [3] (top) and the amplitude model - rotation [2] (bottom) and, choice of best alternative then worst (left) and choice of worst alternative then best (right). The rotation transforms the probability amplitude of the second best choice into the worst choice (left panels), and of the second worst choice into the best choice (right panels). The combinations of chosen alternatives have been consistently colour coded across choice order and models (i.e. red corresponds to Alt₁ as worst, and Alt₂ as best in all four graphs). The ‘basic inversion’ relation, Equation (19), which switches the *residual* probabilities for best (worst) alternative into worst (best) alternative is marked with black dots and serves to gauge the effect of the optimal quantum rotations.

1 combinations of best and worst choice. For instance, the combination Alt₂ worst and Alt₃ best
 2 does not show significant order effects in the amplitude model, nor in the Hamiltonian model. On
 3 the other hand, Alt₁ best and Alt₂ worst is oppositely transformed in both choice orders in the
 4 Hamiltonian model, while on the other hand in the amplitude model Alt₂ best and Alt₁ worst is
 5 oppositely transformed.

6 The optimised proportion parameter has shifted the weight moderately towards the ‘worst then
 7 best’ choice order in both models (order ratio 0.39/0.61 for the Hamiltonian model and 0.36/0.64
 8 for amplitude model). This feature is likely a result of the strong bias in the choice for worst
 9 alternative which would formally be captured more easily by an immediate implementation in the
 10 belief state (for the Amplitude model) and by a dynamical process (in the Hamilton model), than
 11 by a rotation. In the ‘worst then best’ order, both models do not invoke the rotation to render
 12 the probabilities for the worst choice, while in the reverse order ‘best then worst’ the rotation is
 13 involved in the final stage of producing the worst choice probabilities.²⁶

14 To analyse the impact of these rotations in relation to the effects they have on model outputs,
 15 we consider the overall predicted choice shares across the different models (see Table 9).

TABLE 9 : Observed and predicted choice shares from different best-worst models

Best choice		1	1	2	2	3	3	Average deviation
Worst choice		2	3	1	3	1	2	from observed
Utility	[2]	20.4%	14.3%	9.1%	25.8%	6.0%	24.3%	0.5%
DFT	[2]	20.0%	14.3%	9.4%	25.1%	6.3%	24.8%	0.3%
q-Hamiltonian	[3]	20.6%	19.1%	9.9%	19.9%	9.6%	20.8%	3.0%
q-Hamiltonian	[6]	20.1%	14.9%	9.7%	25.0%	6.1%	24.2%	0.2%
q-Amplitude	[3]	20.6%	19.1%	9.8%	20.0%	9.6%	20.9%	2.9%
q-Amplitude	[5]	18.8%	14.5%	11.0%	24.9%	6.1%	24.7%	0.5%
Observed share		19.8%	14.9%	9.8%	25.1%	5.8%	24.6%	

16 The average deviation from the observed choice share of best and worst choice demonstrates the
 17 impact of the quantum rotation on the quantum models with a quantum rotation. Hamiltonian
 18 and amplitude models without a quantum rotation have deviations of 3.0% and 2.9% respectively.
 19 These deviations are substantially reduced by moving to versions of the models with quantum ro-
 20 tations, which brings the results in line with those of the utility and DFT models, with the Hamil-
 21 tonian model in particular almost perfectly capturing the observed choice shares.

22 Finally, we consider the parameter outputs for the best version of each model in Table 10.

23 All four models give the expected sign for all of the attributes. Whilst the relative importance
 24 of the different attributes is similar across the models, there are some exceptions. In particular,
 25 the estimates for travel fare (LF) for the worst choices in the utility and DFT models are very
 26 different, with DFT giving the lowest relative importance to travel fare in both best and worst
 27 choice. DFT gives a higher importance to the rate of delays (RA) and the provision of a free
 28 information service (IFR) than other models. The quantum models provide very similar relative

²⁶Further examination of this order effect could be done in a dataset with explicit choice order specifications in the survey.

TABLE 10 : Parameter estimates from the models for the UK best worst dataset, with rel. weight giving the relative importance of the different attributes.

Model Parameters		Utility		DFT		q-Hamiltonian	q-Amplitude
Log-likelihood		24		26		19	15
BIC		-5,607.63		-5,569.04		-5,633.44	-5,612.08
		11,430		11,371		11,437	11,365
choice		best	worst	best	worst	all	all
LL contribution		-3561.75	-2045.88	-3536.743	-2032.30		
β_{TT}	est.	-0.0259	-0.0221	-0.1942	-0.0414	-0.0096	-0.2716
	rob. t-rat.	-5.96	-3.77	-6.55	-3.56	-9.75	-5.85
	rel. weight	0.5%	0.3%	0.7%	0.5%	0.5%	0.5%
β_{LF}	est.	-5.3428	-7.2843	-25.0410	-7.1054	-1.7815	-46.6046
	rob. t-rat.	-4.78	-6.14	-7.84	-4.31	-9.42	-5.69
	rel. weight	93.0%	93.4%	89.5%	81.6%	91.0%	92.2%
β_{CR}	est.	-0.1235	-0.2333	-0.8419	-0.3671	-0.0506	-1.2673
	rob. t-rat.	-4.43	-4.29	-5.57	-3.77	-8.71	-5.58
	rel. weight	2.2%	3.0%	3.0%	4.2%	2.6%	2.5%
β_{RA}	est.	-0.0778	-0.0019	-0.6702	-0.3897	-0.0506	-0.9285
	rob. t-rat.	-3.19	-2.88	-4.04	-3.22	-4.92	-3.69
	rel. weight	1.4%	0.0%	2.4%	4.5%	2.6%	1.8%
β_{RE}	est.	-0.0042	-0.0077	-0.0290	-0.0098	-0.0016	-0.0435
	rob. t-rat.	-1.47	-1.3%	-2.18	-1.47	-2.56	-2.75
	rel. weight	0.1%	0.1%	0.1%	0.1%	0.1%	0.1%
β_{RB}	est.	-0.0101	-0.0025	-0.0760	-0.0239	-0.0037	-0.0792
	rob. t-rat.	-1.75	-0.18	-2.06	-1.24	-2.08	-2.42
	rel. weight	0.2%	0.0%	0.3%	0.3%	0.2%	0.2%
β_{ICH}	est.	-0.0333	-0.0006	-0.2345	-0.1779	-0.0073	-0.5012
	rob. t-rat.	-1.19	-0.90	-1.06	-0.77	-0.71	-1.98
	rel. weight	0.6%	0.0%	0.8%	2.0%	0.4%	1.0%
β_{IFR}	est.	0.1254	0.2494	0.8986	0.5957	0.0529	0.8245
	rob. t-rat.	4.33	2.7%	4.49	3.49	5.2	3.07
	rel. weight	2.2%	3.2%	3.2%	6.8%	2.7%	1.6%
λ_1	est.	0.3272	5.1126	0.0438	0.4302	1.3547	0.0391
	rob. t-rat.	4.38	3.16	3.31	2.74	11.06	4.56
λ_2	est.	1.8508	0.3102				1.0000
	rob. t-rat.	1.69	7.73				fixed
δ_1	est.	0.0000	0.0000	1.9037	1.2919		2.8439
	rob. t-rat.	fixed	fixed	6.55	5.94		5.79
δ_2	est.	-0.3029	-1.0826	1.1384	-0.9907		8.2458
	rob. t-rat.	-2.69	-14.72	4.09	-5.1		7.05
δ_3	est.	-0.5260	-0.7559	0.0000	0.0000		5.7360
	rob. t-rat.	-4.94	-9.63	fixed	fixed		7.73
δ_{12}	est.					0.0277	
	rob. t-rat.					0.66	
δ_{13}	est.					0.2025	
	rob. t-rat.					9.65	
δ_{23}	est.					-0.1435	
	rob. t-rat.					-5.59	
σ_ε	est.			1.0000	1.0000		
	rob. t-rat.			fixed	fixed		
t	est.			7.1019	5.4830		
	rob. t-rat. (vs. 1)			8.52	4.53		
ϕ_1	est.			0.0040	0.0000		
	rob. t-rat.			2.67	fixed		
ϕ_2	est.			0.3469	0.0000		
	rob. t-rat. (vs. 1)			14.54	fixed		
h_{11}	est.					1.6685	
	rob. t-rat.					34.23	
h_{33}	est.					2.1300	
	rob. t-rat.					20.26	
proportion	est.					0.3943	0.3568
	rob. t-rat.					6.71	7.96
ϑ	est.					1.3718	2.2353
	rob. t-rat. (vs. $\pi/2$)					-5.25	13.82
ω_{BW}	est.					0.1346	1.2641
	rob. t-rat.					2.69	25.85
ω_{WB}	est.					0.2788	
	rob. t-rat.					6.21	
s	est.					1.1709	
	rob. t-rat.					18.43	

1 importances to the utility model. All models suggest that there are differences between best and
 2 worst choice, with both the utility model and DFT in particular finding different sensitivities to
 3 cost when comparing best to worst. Additionally, both find substantially lower estimates for δ_2 in
 4 worst choice compared to best, which is in line with observed choice shares for the 2nd alternative
 5 (best-35%, worst-44%). For the quantum models, we observe angles ϑ , and ω estimates, that
 6 are significantly different from $\pi/2$ and 0 respectively, which would correspond to best being the
 7 opposite of worst for the Hamiltonian model (with ω also significantly different from $\pi/2$ for the
 8 amplitude model, equivalently demonstrating that it too suggests that best is not the opposite of
 9 worst).

10 5.5. Validation results: Holdout method

11 We also test for overfitting, by testing the best performing model (in terms of BIC) for each of the
 12 four different types of model in our best-worst data. This corresponds to a separate parameters
 13 model for the utility and DFT models, and to models with quantum rotations and a proportion
 14 parameter for the Hamiltonian and amplitude models (2 rotations for the Hamiltonian, but just one
 15 for the amplitude model). We fit the data to 5 estimation subsets and then estimate the out-of-
 16 sample log-likelihood for the remaining validation subset. In each case, 80% of the (participants
 17 in the) dataset are assigned to the subset that is used for model estimation, with the remaining 20%
 18 used for validation. The log-likelihoods of these models are given in Table 11.

TABLE 11 : The log-likelihood results for the estimation and holdout samples for the different models for the UK best-worst dataset

	Utility		DFT		q-Hamiltonian		q-Amplitude	
	pars.	LL	pars.	LL	pars.	LL	pars.	LL
estimation 1	24	-4,508.98	26	-4,471.93	19	-4,522.45	15	-4,519.58
estimation 2	24	-4,420.34	26	-4,394.00	19	-4,439.09	15	-4,412.87
estimation 3	24	-4,526.41	26	-4,498.69	19	-4,540.49	15	-4,529.31
estimation 4	24	-4,486.07	26	-4,462.50	19	-4,500.03	15	-4,498.81
estimation 5	24	-4,468.13	26	-4,426.69	19	-4,480.68	15	-4,472.40
holdout 1	24	-1,106.20	26	-1,104.27	19	-1,106.51	15	-1,097.21
holdout 2	24	-1,193.77	26	-1,183.34	19	-1,190.84	15	-1,205.68
holdout 3	24	-1,084.95	26	-1,073.84	19	-1,086.96	15	-1,084.99
holdout 4	24	-1,125.21	26	-1,110.85	19	-1,127.82	15	-1,117.01
holdout 5	24	-1,143.46	26	-1,148.45	19	-1,146.99	15	-1,141.51

19 The results suggest that neither the quantum models nor DFT overfit the data, with DFT giving
 20 the best fit in all 5 estimation and 3 of the validation subsets, and the amplitude model having the
 21 best fit in the other two validation subsets. The BIC values for these models are given in Figure
 22 9, which penalises the utility and DFT models. This consequently results in the amplitude model
 23 obtaining the best BIC value across all 5 estimation and validation subsets.

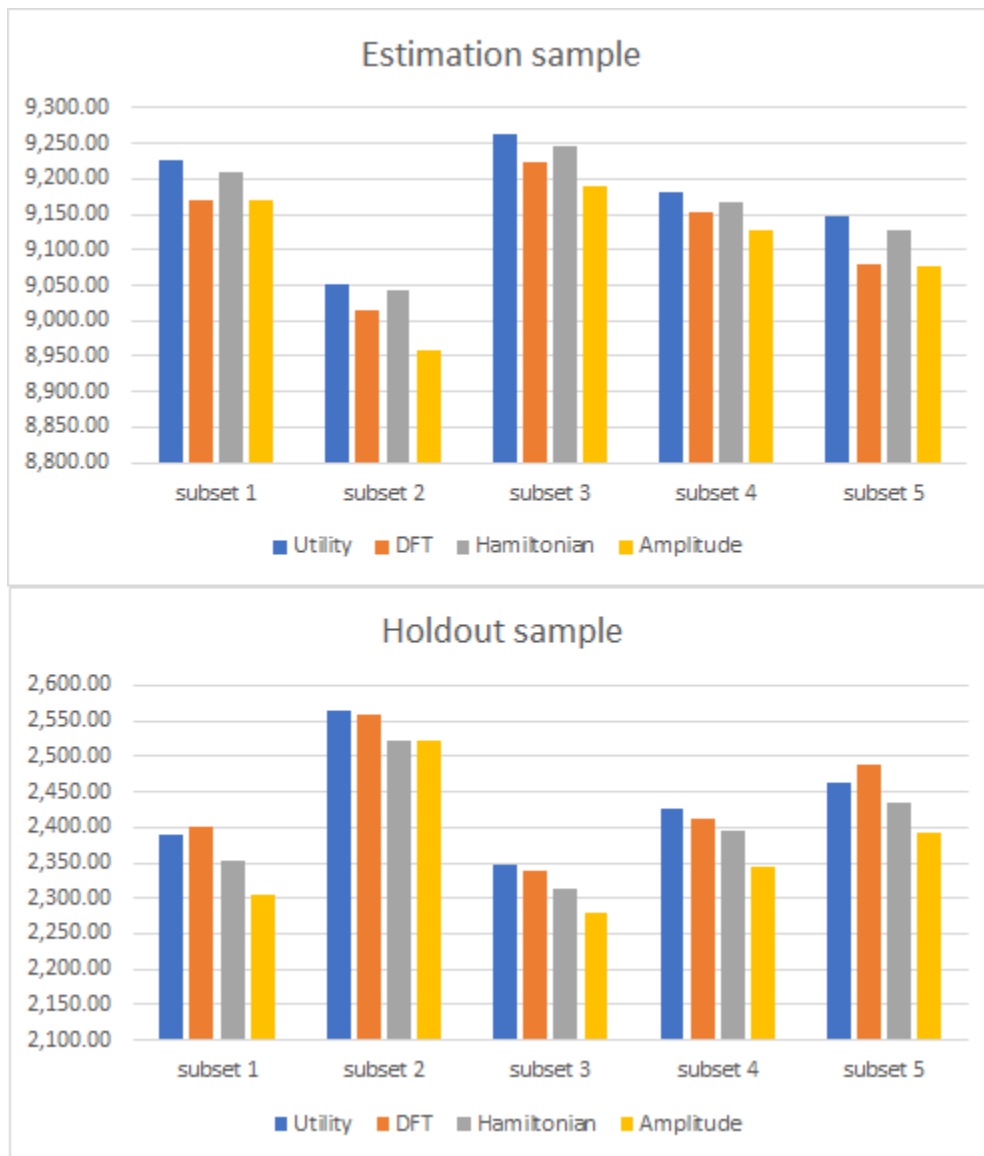


FIGURE 9 : The BIC results for the estimation and holdout samples for the different models for the UK best-worst dataset

1 5.6. Elasticities from value of time datasets

2 In this section, we look at elasticities from the best version of each model (in terms of BIC) for the
 3 Swiss value of time and UK value of time datasets. For all models, we estimate an arc elasticity
 4 (E) for alternative i with:

$$E_i = \log \left(\frac{\text{Forecasted Trips}_i}{\text{Base Trips}_i} \right) / \log(1.1), \quad (40)$$

5 where ‘Base Trips $_i$ ’ is calculated as the sum over the probabilities of choosing alternative i across
 6 all choice tasks in the dataset, with ‘Forecasted Trips $_i$ ’ calculated equivalently but with adjusted
 7 attributes. The corresponding cross elasticities, CE_j , estimate the impact on the probability of
 8 choosing alternative j given a change to an attribute of alternative i . We estimate elasticities by
 9 using a 10% increase of the controlling factor (see Equation 40), either travel time or travel cost
 10 for alternative 1, with the results given in Table 12. We estimate standard errors for the elasticities
 11 by taking 30 draws for the parameter values from the corresponding model estimates and robust
 12 covariance matrices.

TABLE 12 : Arc elasticities for an increase in travel time or travel cost for the first alternative in the value of time datasets

UK Value of Time dataset						
	arc elasticities for cost (alt1)			arc elasticities for time (alt1)		
	est	s.d.	t-value (vs utility)	est	s.d.	t-value (vs utility)
Utility	-1.5600	0.0617		-2.0476	0.0393	
DFT	-1.7962	0.0488	-3.00	-2.2205	0.0467	-2.83
q-Hamiltonian	-0.9335	0.0564	7.49	-1.6876	0.0766	4.18
q-Amplitude	-1.8411	0.0473	-3.62	-2.4337	0.0647	-5.10
Swiss Value of Time dataset						
	arc elasticities for cost (alt1)			arc elasticities for time (alt1)		
	est	s.d.	t-value (vs utility)	est	s.d.	t-value (vs utility)
Utility	-1.6641	0.2380		-1.4043	0.1241	
DFT	-1.6304	0.1406	0.12	-1.3705	0.0773	0.23
q-Hamiltonian	-1.3034	0.1700	1.23	-1.1648	0.0890	1.57
q-Amplitude	-1.7363	0.1454	-0.26	-1.4199	0.0948	-0.10

13 For the UK dataset, we observe significantly lower elasticities for the Hamiltonian model, and
 14 significantly higher elasticities for the amplitude model (relative to the utility model). There are
 15 equivalent results for both cost and time elasticities, with the amplitude and Hamiltonian models
 16 predicting greater and smaller shifts, respectively, away from choosing alternative 1 if the cost or
 17 time increases, relative to the utility model. For the Swiss dataset, we observe similar patterns to
 18 the UK dataset for the quantum models, but these differences are never significant. The elasticities
 19 from all models are higher than would be expected, though this is of course typical for SP datasets.
 20 Overall, the elasticities from the best performing quantum model (the amplitude model) appear
 21 reasonable in comparison to the elasticities given by the utility model.

1 6. CONCLUSIONS

2 In this paper, we move away from the tried and tested alternatives to random utility maximisation
3 by considering ideas first developed in quantum physics. With the probability framework devel-
4 oped in quantum physics having made a successful transition to cognitive psychology, we look at
5 whether it can be operationalised into a choice model framework for transportation studies. Under
6 quantum probability theory, a decision-maker has some ‘belief state’ regarding their preferences
7 over alternatives, from which the probabilities of each alternative can be inferred. Thus a key com-
8 ponent of this paper is the development of specifications for the belief state and how these beliefs
9 change through the process of decision making.

10 We discuss two very different formulations for models generating belief states which incor-
11 porate quantum probability theory within a choice model. The first uses a Hamiltonian operator
12 that dynamically evolves the belief state over time. The second is based on directly estimating the
13 probability amplitudes of the belief state for each of the alternatives. We find that our quantum
14 models provide good model fit and outperform standard utility-based models across three route
15 choice datasets as well as providing good out-of-sample fit for the most complex of these. In com-
16 parison to Decision Field Theory (DFT), which has also been shown to outperform standard choice
17 models (Hancock, 2019), our quantum models also perform favourably, with the amplitude models
18 recording the best BIC values across all datasets. Additionally, we find good model performance
19 from our quantum Hamiltonian model, although it appears that in the particular choice contexts we
20 test it, the quantum amplitude model performs better. These positive results from our initial tests
21 on quantum choice models suggest that there is ample scope for models with a quantum framework
22 to be used within travel behaviour modelling.

23 In order to perform fair tests of our quantum choice models against utility-based models and
24 Decision Field Theory, we discuss four different value functions that are used to implement the
25 attribute differences into the choice models. Overall, it often appears that the value functions
26 themselves have a larger impact on model results than the model structure, with the ADLD models
27 for the UK value of time data in particular giving very similar log-likelihoods across models with
28 vastly different paradigms. However, with the exception of linear difference models, it appears
29 that our quantum amplitude model tends to outperform the utility-based models. This exploration
30 of different value functions also leads to the development of a first DFT model which specifically
31 implements non-linear attribute differences. This results in a significant improvement in our DFT
32 model across all datasets, with a substantial improvement recorded for the UK value of time dataset
33 in particular.

34 A key benefit of the quantum amplitude model over DFT is that it is simple to run and estimate,
35 meaning that it could be applied to a wide range of choice scenarios. However, for these models to
36 make a transition into large-scale modelling, an alternative specification would need to be defined
37 to avoid the same pitfall of random regret minimisation for large numbers of alternatives: using
38 a comparison between every pair of alternatives quickly becomes computationally infeasible and
39 quantum amplitude models with linear attribute differences perform worse than standard multinomial
40 logit models. Another issue with the current specifications of the quantum models is that it
41 could be argued that it is unclear how specifically the use of real and imaginary numbers improves
42 the quantum models, with further work being required to understand the mechanisms at work here.
43 Additionally, by restricting the belief state to be defined by the value functions tested in this paper,
44 we deny the possibility of having a probabilistic belief state, as conceptualised by quantum theory.
45 This limitation can easily be addressed through the incorporation of random parameters for the rel-

1 ative importance of the different attributes, which would naturally allow for a probabilistic belief
2 state.

3 That being noted, the results from our quantum rotation models in this paper suggest that
4 there is potentially a wide range of benefits of bringing quantum probability theory into choice
5 models. Crucially, our best performing models for the best-worst dataset and the contextual choice
6 dataset, after allowing for model complexity to be taken into account, are the amplitude models
7 including a quantum rotation. This suggests that there is some merit in the concept of quantum
8 rotation, which indicates a different set of basis vectors for choices are required for different choice
9 tasks. For example, the belief state rotation works well for capturing the difference between best
10 and worst choice. Despite the fact that the best-worst choices are related, the quantum rotation
11 suggests that these choices are in fact incompatible: the choices cannot be made at the same time
12 and consequently they may not follow the classical probability law of distributivity. This means
13 that different choices may be observed depending on whether the decision-maker chooses the best
14 or worst alternative first. The use of such information may also provide a number of insights for
15 better specifications of quantum models that incorporate ‘best then worst’ or ‘worst then best’
16 deliberation processes. An enhanced implementation of our quantum approach demonstrated and
17 improved model performance by integrating both orderings of the choice process, ‘best then worst’
18 and ‘worst then best’.

19 While the quantum rotation findings here are just illustrative examples, these results demon-
20 strate that there is major scope for future work within travel behaviour modelling. For example,
21 large-scale models frequently aim to understand a series of related, sequential choices. Given the
22 ability of quantum rotations to capture the translation between best and worst choices, they the-
23 oretically should also work for a larger sequence of related choices where continuously adding
24 on separate sets of parameters may not be possible. Ordering effects and state dependence may
25 thus be well captured by models within a quantum framework. Furthermore, it may be possible
26 to mitigate the impacts of contextual effects by applying the appropriate quantum rotation derived
27 from other quantum models that account for the same effect. Future efforts could also compare
28 quantum frameworks against other models that are specifically designed to deal with contextual
29 effects, such as prospect theory or MLBA. Additionally, quantum choice models could be applied
30 to experimental paradigms in which a nudge is involved in some of the choice tasks (for example, a
31 scenario such as the environmentalism example discussed in the introduction of this paper). These
32 future possibilities combined with the positive results in our empirical work mean that this paper
33 serves as a proof-of-concept that quantum ideas can be incorporated into choice models aiming to
34 understand travel behaviour.

35 **ACKNOWLEDGEMENTS**

36 The authors are grateful to four anonymous referees as well as Tony Marley for helpful suggestions
37 on an earlier version of this paper. The authors would also like to acknowledge the financial support
38 by the European Research Council through the consolidator grant 615596-DECISIONS.

1 **REFERENCES**

- 2 Aerts, D., Broekaert, J., and Smets, S. (1999). A quantum structure description of the liar paradox.
3 International Journal of Theoretical Physics, 38(12):3231–3239.
- 4 Aerts, D. and Gabora, L. (2005). A theory of concepts and their combinations ii: A hilbert space
5 representation. Kybernetes.
- 6 Asano, M., Khrennikov, A., Ohya, M., Tanaka, Y., and Yamato, I. (2015). Quantum Adaptivity in
7 Biology: From Genetics to Cognition. Springer Netherlands.
- 8 Atmanspacher, H. and Filk, T. (2010). A proposed test of temporal nonlocality in bistable percep-
9 tion. Journal of Mathematical Psychology, 54(3):314–321.
- 10 Avineri, E. and Bovy, P. H. (2008). Identification of parameters for a prospect theory model for
11 travel choice analysis. Transportation Research Record, 2082(1):141–147.
- 12 Axhausen, K. W., Hess, S., König, A., Abay, G., Bates, J. J., and Bierlaire, M. (2008). Income
13 and distance elasticities of values of travel time savings: New swiss results. Transport Policy,
14 15(3):173–185.
- 15 Bagarello, F. (2019). Quantum Concepts in the Social, Ecological and Biological Sciences. Cam-
16 bridge University Press.
- 17 Batley, R., Bates, J., Bliemer, M., Börjesson, M., Bourdon, J., Cabral, M. O., Chintakayala, P. K.,
18 Choudhury, C., Daly, A., Dekker, T., et al. (2017). New appraisal values of travel time saving
19 and reliability in great britain. Transportation, pages 1–39.
- 20 Batley, R. and Dekker, T. (2019). The intuition behind income effects of price changes in discrete
21 choice models, and a simple method for measuring the compensating variation. Environmental
22 and Resource Economics, 74(1):337–366.
- 23 Ben-Akiva, M., McFadden, D., Train, K., et al. (2019). Foundations of stated preference elici-
24 tation: Consumer behavior and choice-based conjoint analysis. Foundations and Trends® in
25 Econometrics, 10(1-2):1–144.
- 26 Bierlaire, M., Thémans, M., and Zufferey, N. (2010). A heuristic for nonlinear global optimization.
27 INFORMS Journal on Computing, 22(1):59–70.
- 28 Birkhoff, G. and Von Neumann, J. (1936). The logic of quantum mechanics. Annals of
29 mathematics, pages 823–843.
- 30 Blumenson, L. E. (1960). A derivation of n-dimensional spherical coordinates. The American
31 Mathematical Monthly, 67(1):63–66.
- 32 Broekaert, J., Basieva, I., Blasiak, P., and Pothos, E. M. (2017). Quantum-like dynamics applied to
33 cognition: a consideration of available options. Philosophical Transactions of the Royal Society
34 A, 375.
- 35 Broekaert, J., Busemeyer, J., and Pothos, E. (2020). The disjunction effect in two-stage simulated
36 gambles. an experimental study and comparison of a heuristic logistic, markov and quantum-like
37 model. Cognitive Psychology, 117:101262.
- 38 Brown, S. D. and Heathcote, A. (2008). The simplest complete model of choice response time:
39 Linear ballistic accumulation. Cognitive Psychology, 57(3):153–178.
- 40 Bruza, P. D., Wang, Z., and Busemeyer, J. R. (2015). Quantum cognition: a new theoretical
41 approach to psychology. Trends in cognitive sciences, 19(7):383–393.
- 42 Busemeyer, J. R. and Bruza, P. D. (2012). Quantum Models of Cognition and Decision. Cambridge
43 University Press.
- 44 Busemeyer, J. R., Pothos, E. M., Franco, R., and Trueblood, J. S. (2011). A quantum theoretical
45 explanation for probability judgment errors. Psychological review, 118(2):193.

- 1 Busemeyer, J. R. and Townsend, J. T. (1992). Fundamental derivations from decision field theory.
2 Mathematical Social Sciences, 23(3):255–282.
- 3 Busemeyer, J. R. and Townsend, J. T. (1993). Decision field theory: a dynamic-cognitive approach
4 to decision making in an uncertain environment. Psychological Review, 100(3):432.
- 5 Busemeyer, J. R., Wang, Z., and Lambert-Mogiliansky, A. (2009). Empirical comparison of
6 markov and quantum models of decision making. Journal of Mathematical Psychology,
7 53(5):423–433.
- 8 Busemeyer, J. R., Wang, Z., and Townsend, J. T. (2006). Quantum dynamics of human decision-
9 making. Journal of Mathematical Psychology, 50(3):220–241.
- 10 Chorus, C. G. (2010). A new model of random regret minimization. EJTIR, 10(2).
- 11 Chorus, C. G., Arentze, T. A., and Timmermans, H. J. (2008). A random regret-minimization
12 model of travel choice. Transportation Research Part B: Methodological, 42(1):1–18.
- 13 Cohen, A. L., Kang, N., and Leise, T. L. (2017). Multi-attribute, multi-alternative models of
14 choice: Choice, reaction time, and process tracing. Cognitive Psychology, 98:45–72.
- 15 Cunha-e Sá, M. A., Madureira, L., Nunes, L. C., and Otrachshenko, V. (2012). Protesting and
16 justifying: a latent class model for contingent valuation with attitudinal data. Environmental
17 and Resource Economics, 52(4):531–548.
- 18 Daly, A. and Hess, S. (2010). Simple approaches for random utility modelling with panel data. In
19 European Transport Conference. Citeseer.
- 20 Dekker, T. (2014). Indifference based value of time measures for random regret minimisation
21 models. Journal of choice modelling, 12:10–20.
- 22 Dugas, C., Bengio, Y., Bélisle, F., Nadeau, C., and Garcia, R. (2001). A universal approximator of
23 convex functions applied to option pricing. Advances in Neural Information Processing Systems,
24 13:1–8.
- 25 Englert, B.-G. (1996). Fringe visibility and which-way information: An inequality. Phys. Rev.
26 Lett., 77(11):2154–2157.
- 27 Feynman, R. P., Leighton, R. B., and Sands, M. (1965). The Feynman Lectures on Physics - III.
28 Addison-Wesley.
- 29 Fuss, I. and Navarro, D. (2013). Open parallel cooperative and competitive decision processes:
30 A potential provenance for quantum probability decision models. Topics in Cognitive Science,
31 5:818–843.
- 32 Giergiczny, M., Dekker, T., Hess, S., and Chintakayala, P. K. (2017). Testing the stability of
33 utility parameters in repeated best, repeated best-worst and one-off best-worst studies. European
34 Journal of Transport and Infrastructure Research, 17(4).
- 35 Greenberger, D. M. and Yasin, A. (1988). Simultaneous wave and particle knowledge in a neutron
36 interferometer. Phys. Lett. A., 128(8):391–394.
- 37 Guevara, C. A. and Fukushi, M. (2016). Modeling the decoy effect with context-rum models:
38 Diagrammatic analysis and empirical evidence from route choice sp and mode choice rp case
39 studies. Transportation Research Part B: Methodological, 93:318–337.
- 40 Hahnloser, R., Sarpeshkar, R., Mahowald, M. A., Douglas, R. J., and Seung, H. S. (2000). Dig-
41 ital selection and analogue amplification coexist in a cortex-inspired silicon circuit. Nature,
42 405:947–951.
- 43 Hancock, T. O. (2019). Travel behaviour modelling at the interface between econometrics and
44 mathematical psychology. PhD thesis, University of Leeds.

- 1 Hancock, T. O., Hess, S., and Choudhury, C. F. (2018). Decision field theory: Improvements to cur-
2 rent methodology and comparisons with standard choice modelling techniques. Transportation
3 Research Part B: Methodological, 107:18–40.
- 4 Hancock, T. O., Hess, S., Marley, A. A. J., and Choudhury, C. F. (2020). An accumulation of
5 preference: two alternative dynamic models for understanding transport choices. Submitted.
- 6 Hawkins, G. E., Islam, T., and Marley, A. (2019). Like it or not, you are using one value represen-
7 tation. Decision, 6(3):237–260.
- 8 Henningsen, A. and Toomet, O. (2011). maxlik: A package for maximum likelihood estimation in
9 R. Computational Statistics, 26(3):443–458.
- 10 Hess, S., Daly, A., and Batley, R. (2018). Revisiting consistency with random utility maximisation:
11 theory and implications for practical work. Theory and Decision, 84(2):181–204.
- 12 Hess, S., Daly, A., Dekker, T., Cabral, M. O., and Batley, R. (2017). A framework for capturing
13 heterogeneity, heteroskedasticity, non-linearity, reference dependence and design artefacts in
14 value of time research. Transportation Research Part B: Methodological, 96:126–149.
- 15 Hess, S. and Palma, D. (2019). Apollo: A flexible, powerful and customisable freeware package
16 for choice model estimation and application. Journal of Choice Modelling, 32:100170.
- 17 Hess, S., Rose, J. M., and Hensher, D. A. (2008). Asymmetric preference formation in willing-
18 ness to pay estimates in discrete choice models. Transportation Research Part E: Logistics and
19 Transportation Review, 44(5):847–863.
- 20 Hotelling, J. M., Busemeyer, J. R., and Li, J. (2010). Theoretical developments in decision field
21 theory: comment on Tsetsos, Usher, and Chater (2010). Psychological Review, 117(4):1294–
22 1298.
- 23 Hughes, R. I. (1992). The structure and interpretation of quantum mechanics. Harvard university
24 press.
- 25 Kempe, J. (2003). Quantum random walks: an introductory overview. Contemporary Physics,
26 44(4):307–327.
- 27 Krajbich, I., Lu, D., Camerer, C., and Rangel, A. (2012). The attentional drift-diffusion model
28 extends to simple purchasing decisions. Frontiers in Psychology, 3:193.
- 29 Kvam, P. D., Pleskac, T. J., Yu, S., and Busemeyer, J. R. (2015). Interference effects of choice
30 on confidence: Quantum characteristics of evidence accumulation. Proceedings of the National
31 Academy of Sciences, 112(34):10645–10650.
- 32 Leong, W. and Hensher, D. A. (2014). Relative advantage maximisation as a model of context
33 dependence for binary choice data. Journal of choice modelling, 11:30–42.
- 34 Lipovetsky, S. (2018). Quantum paradigm of probability amplitude and complex utility in entan-
35 gled discrete choice modeling. Journal of choice modelling, 27:62–73.
- 36 Mahieu, P.-A., Crastes, R., Louviere, J., Zawojka, E., et al. (2016). Rewarding truthful-telling
37 in stated preference studies. Technical report, Faculty of Economic Sciences, University of
38 Warsaw.
- 39 Martínez-Martínez, I. (2014). A connection between quantum decision theory and quantum games:
40 The hamiltonian of strategic interaction. Journal of Mathematical Psychology, 58:33–44.
- 41 Masiero, L. and Hensher, D. A. (2010). Analyzing loss aversion and diminishing sensitivity in a
42 freight transport stated choice experiment. Transportation Research Part A: Policy and Practice,
43 44(5):349–358.
- 44 McFadden, D. (1974). Conditional Logit Analysis of Qualitative Choice Behaviour.
45 In Frontiers in Econometrics, ed. P. Zarembka. (New York: Academic Press).

- 1 Moreira, C. and Wichert, A. (2016). Quantum probabilistic models revisited: The case of disjunc-
2 tion effects in cognition. *Frontiers in Physics*, 4:26.
- 3 Nair, V. and Hinton, G. E. (2010). Rectified linear units improve restricted boltzmann machines. In
4 *Proceedings of the 27th international conference on machine learning (ICML-10)*, pages 807–
5 814.
- 6 Pothos, E. M. and Busemeyer, J. R. (2009). A quantum probability explanation for viola-
7 tions of ‘rational’ decision theory. *Proceedings of the Royal Society B: Biological Sciences*,
8 276(1665):2171–2178.
- 9 Pothos, E. M., Busemeyer, J. R., and Trueblood, J. S. (2013). A quantum geometric model of
10 similarity. *Psychological Review*, 120(3):679.
- 11 Roe, R. M., Busemeyer, J. R., and Townsend, J. T. (2001). Multialternative decision field theory:
12 A dynamic connectionist model of decision making. *Psychological Review*, 108(2):370.
- 13 Seetharaman, P. (2003). Probabilistic versus random-utility models of state dependence: an em-
14 pirical comparison. *International Journal of Research in Marketing*, 20(1):87–96.
- 15 Stathopoulos, A. and Hess, S. (2012). Revisiting reference point formation, gains–losses asymme-
16 try and non-linear sensitivities with an emphasis on attribute specific treatment. *Transportation*
17 *Research Part A: Policy and Practice*, 46(10):1673–1689.
- 18 Train, K. (2003). Discrete choice with simulation.
- 19 Trueblood, J. S., Brown, S. D., and Heathcote, A. (2014a). The multiattribute linear ballistic accu-
20 mulator model of context effects in multialternative choice. *Psychological review*, 121(2):179–
21 205.
- 22 Trueblood, J. S. and Busemeyer, J. R. (2011). A quantum probability account of order effects in
23 inference. *Cognitive science*, 35(8):1518–1552.
- 24 Trueblood, J. S. and Busemeyer, J. R. (2012). Quantum information processing theory. In
25 *Encyclopedia of the Sciences of Learning*, pages 2748–2751. Springer.
- 26 Trueblood, J. S., Pothos, E. M., and Busemeyer, J. R. (2014b). Quantum probability theory as a
27 common framework for reasoning and similarity. *Frontiers in psychology*, 5:322.
- 28 Turner, B. M., Schley, D. R., Muller, C., and Tsetsos, K. (2018). Competing theories of multial-
29 ternative, multiattribute preferential choice. *Psychological Review*, 125(3):329.
- 30 Tversky, A. (1977). Features of similarity. *Psychological Review*, 84(4):327.
- 31 van Cranenburgh, S., Guevara, C. A., and Chorus, C. G. (2015). New insights on random regret
32 minimization models. *Transportation Research Part A: Policy and Practice*, 74:91–109.
- 33 van Rijsbergen, C. (2004). *The Geometry of Information Retrieval*. Cambridge.
- 34 Vitetta, A. (2016). A quantum utility model for route choice in transport systems. *Travel Behaviour*
35 *and Society*, 3:29–37.
- 36 White, L. C., Pothos, E. M., and Busemeyer, J. R. (2014). Sometimes it does hurt to ask: The
37 constructive role of articulating impressions. *Cognition*, 133(1):48–64.
- 38 Yu, J. G. and Jayakrishnan, R. (2018). A quantum cognition model for bridging stated and revealed
39 preference. *Transportation Research Part B: Methodological*, 118:263–280.
- 40 Zheng, H., Yang, Z., Liu, W., Liang, J., and Li, Y. (2015). Improving deep neural networks using
41 softplus units. In *2015 International Joint Conference on Neural Networks (IJCNN)*, pages 1–4.
42 IEEE.

1 APPENDIX: COMPARATIVE MODELS

2 **The logit model.** We test our quantum models against standard choice models (McFadden, 1974;
3 Train, 2003; Ben-Akiva et al., 2019) using the same value functions. For these models, we define
4 the utility for an alternative i (dropping the indices for individual (n) and choice task (t)) as:

$$V_i = \varepsilon_i + \sum_{j \neq i} \Delta_{ij}, \quad (\text{A1})$$

5 where Δ_{ij} is defined using one of the four value functions and ε_i is the unobserved portion of the
6 utility.²⁷ The assumption of type I extreme value distributions results in typical probabilities:

$$P_i = \frac{e^{V_i}}{\sum_{j=1}^J e^{V_j}}, \quad (\text{A2})$$

7 for each individual (n) and choice task (t). Using this function together with the regret-based value
8 functions would of course result in the wrong signs for the β -coefficients, thus we use $-V_i$ and
9 $-V_j$ instead of V_i and V_j for these models. As we do not have this transformation in the quantum
10 models, they instead use Δ_{ji} in place of Δ_{ij} to ensure the correct sign for the β -coefficients.

11 **Decision Field Theory.** We also test DFT, which was originally developed within mathemati-
12 cal psychology (Busemeyer and Townsend, 1992, 1993), thus is very different to models based on
13 econometric theory. The key assumption under a DFT model is that each alternative has a prefer-
14 ence value that updates over time within a single choice context. The decision-maker considers the
15 alternatives until they reach some internal threshold (similar to the concept of satisficing, where
16 one of the alternatives is deemed ‘good enough’) or an external threshold (i.e. some time con-
17 straint, where a decision-maker stops deliberating on the alternatives as a result of running out of
18 time to make the decision). An example of a decision process under DFT is given in Figure A1.

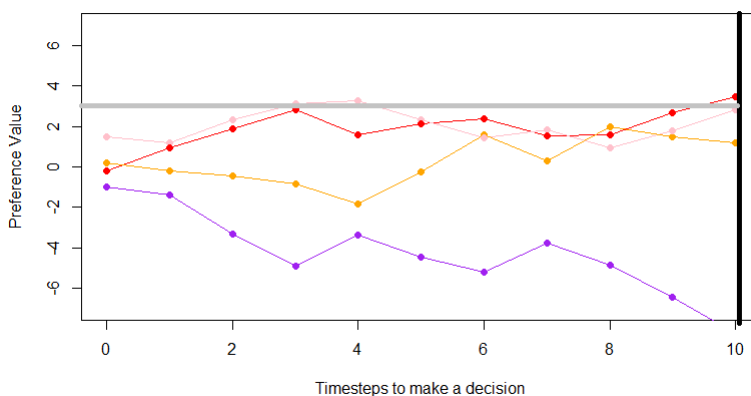


FIGURE A1 : An example of a decision-maker stopping upon reaching either an internal or external threshold

19 In the example given in this figure, the decision-maker chooses different alternatives if they make
20 their choice after reaching an internal threshold (which is represented by the horizontal line) on
21 the 4th preference updating step or if they conclude after 10 steps upon reaching a time threshold.

²⁷Note that this is equivalent to the specification of the probability amplitude, ψ_i in Equation 3.

1 Mathematically, DFT was originally operationalised for internal thresholds, with a full account
 2 of this variation of DFT given by [Busemeyer and Townsend \(1993\)](#). However, the DFT models
 3 we use in this paper is based on DFT with external thresholds (c.f. [Roe et al. \(2001\)](#) for the
 4 first version of DFT with external thresholds for multiple alternatives). For DFT with an external
 5 threshold, the preference values update stochastically as a result of the assumption that a decision-
 6 maker compares the alternatives using just a single attribute at each preference updating step.
 7 Consequently, the preference values for the alternatives update iteratively:

$$P_t = S \cdot P_{t-1} + V_t, \quad (\text{A3})$$

8 where P_t is a column vector containing the preference values of each alternative i at time t . S is
 9 a feedback matrix with memory and sensitivity parameters (detailed in Equation [A4](#)) and V_t is a
 10 valence vector (Equation [A5](#)), which varies depending on which attribute is attended to at time t ,
 11 and is equivalent to a ‘momentary utility’. The feedback matrix we use is based on the definition
 12 by [Hotelling et al. \(2010\)](#):

$$S = I - \phi_2 \times \exp(-\phi_1 \times D^2), \quad (\text{A4})$$

13 where I is an identity matrix of size n , where n is the number of alternatives. The feedback
 14 parameter has two free parameters. The first, ϕ_1 , is a ‘sensitivity’ parameter, which allows for
 15 competition between alternatives that are more similar (in terms of attribute values). This is the
 16 driving force that results in DFT being able to account for contextual effects ([Roe et al., 2001](#)). The
 17 second parameter, ϕ_2 is a ‘memory’ parameter, which captures whether attributes considered at the
 18 start of the deliberation process or attributes considered at the end are more important. Crucially,
 19 a value of $\phi_2 = 0$ results in the feedback matrix collapsing to an identity matrix, meaning that ‘no
 20 memory loss’ results in it not being possible for ϕ_1 to have an impact. This means that ϕ_2 has
 21 an important mathematical role in the model and thus cannot be purely treated as a psychological
 22 parameter, which is especially the case when DFT is applied to choice-only data. Finally, D is
 23 some measure of distance between the alternatives. In this paper, we use the Euclidean distance
 24 for simplicity. Next, the valence vector can be described:

$$V_t = C \cdot M \cdot W_t + \varepsilon_t, \quad (\text{A5})$$

25 where C is a contrast matrix used to rescale the attribute values such that they total zero, M is a
 26 matrix containing the attribute values for all of the alternatives, $W_t = [0..1..0]'$ is a column vector
 27 and ε_t is an error term. W_t defines which attribute is being attended to by the decision-maker
 28 at preference updating step t , with entry $k = 1$ if and only if attribute k is the attended attribute.
 29 Note that the DFT models in this paper follow the new attribute scaling method developed by
 30 [Hancock et al. \(2020\)](#). Instead of estimating attribute importance weights, w_k , that corresponds
 31 to the likelihood of a decision-maker attending to that attribute k , we estimate ‘attribute scaling
 32 coefficients’. These have many benefits (see [Hancock et al. \(2020\)](#) for a detailed explanation of
 33 these), including, most importantly, avoiding the limitation of having to sum to one. By instead
 34 assuming that each attribute is attended to with the same likelihood (all weights, $w_k = 1/n$), the
 35 relative importance can instead enter as a set of scaling coefficients, β_k , which are applied to the
 36 attributes before they are entered (through M in Equation [A5](#)) into the calculation of the valence
 37 vector at each preference updating step.

38 Finally, the error term is drawn from independent and identically distributed normal draws
 39 with mean 0 and a standard deviation, σ_ε , which is an estimated parameter. Consequently, the

1 preference values P_t converge to a multivariate normal distribution (Roe et al., 2001). To calculate
 2 the probability with which each alternative is chosen under decision field theory, we simply require
 3 the expectation and covariance of P_t (ξ_t and Ω_t , respectively, detailed in Hancock et al. 2018).
 4 Hence the probability of choosing alternative j from a set of J alternatives at time t is:

$$Pr_j \left[\max_{i \in J} P_t [i] = P_t [j] \right] = \int_{X>0} \exp \left[-(X - \Gamma)' \Lambda^{-1} (X - \Gamma) / 2 \right] / (2\pi |\Lambda|^{0.5}) dX, \quad (A6)$$

5 with X the set of differences between the preference value for the chosen alternative and each
 6 other alternative, $X = [P_t [j] - P_t [1], \dots, P_t [j] - P_t [J]]'$. Additionally, we require transformations of
 7 the expectation and covariance, $\Gamma = L\xi_t$, $\Lambda = L\Omega_t L'$, with L a matrix comprised of a column vector
 8 of 1s and a negative identity matrix of size $J - 1$ where J is the number of alternatives. The column
 9 vector of 1s is placed in the i^{th} column where i is the chosen alternative.

10 Prior to this paper (as far as the authors are aware), DFT has always been implemented using
 11 linear attribute differences, which are enforced by the contrast matrix, C . This results in element j
 12 of the matrix $C \cdot M \cdot W_t$ taking the form:

$$CMW_t [j] = \sum_1^n \frac{\beta_k (x_{jk} - x_{ik})}{n}, \quad (A7)$$

13 where n is the number of alternatives as before and k is the attribute being attended to at preference
 14 updating step t . Given that the value functions incorporating a softplus function do not result in
 15 $\Delta_{ij} = \Delta_{ji}$, they are not appropriate functions to be used within a DFT model. This is because
 16 DFT models use just a single difference Δ_{ij} , thus it is unclear whether Δ_{ij} or Δ_{ji} should be used.
 17 However, our ADLD value function can be configured such that $\Delta_{ij} = \Delta_{ji}$, if $\lambda_1 = \lambda_2$. Thus our
 18 ADLD DFT models require just a single λ parameter. The element $CMW_t [j]$ can thus have an
 19 updated numerator based on the ADLD value function:

$$CMW_t [j] = \sum_1^n \frac{\exp(-\lambda \cdot \beta_k \cdot |x_{jk} - x_{ik}|) \cdot \beta_k \cdot (x_{jk} - x_{ik})}{n}. \quad (A8)$$

20 It is worth noting here that we do not sum across attributes for each preference updating step,
 21 though to calculate the expectation of the preference values after t steps, a summation is required.